

SECTION III

TITLE PAGES OF PUBLISHED PAPERS

(JULY 1978-JUNE 1979)

Observation of the $T_> = \frac{45}{2}$ Components of Deep Hole States in ^{207}Pb via the $(^3\text{He}, \alpha)$ Reaction at 70 MeV

S. Gales,^(a) G. M. Crawley, D. Weber, and B. Zwieglinski^(b)

Cyclotron Laboratory, Michigan State University, East Lansing, Michigan 48824

(Received 12 May 1978)

A number of narrow lines are observed around 20 MeV excitation energy in ^{207}Pb in the study of $^{208}\text{Pb}(^3\text{He}, \alpha)$ at 70 MeV. Their excitation energies and relative spacing suggest that these peaks arise from the neutron pickup from the inner filled $sdhg$ shell between magic numbers 82 and 50 with isospin number $T = \frac{45}{2}$. In addition, distorted-wave Born-approximation (DWBA) calculations of the angular distributions agree in shape with the data. The solution of the Lane coupled-channels equations leads to a DWBA cross section in reasonable agreement with experiment.

In the past few years a number of experiments have been carried out in heavy nuclei in order to locate the $T_<$ components of inner hole states using neutron pickup reactions.¹⁻⁹ In general, both the $T_<$ and the $T_>$ components of these inner neutron hole states are populated, the latter ($T_>$) observed as sharp peaks at high excitation energy above a continuous background.^{4,5,8-10} These studies are of importance because they provide quantitative information on the spreading of simple configurations into the underlying background in a region of very high level density. A simple calculation of the Coulomb displacement energy predicts that these levels are located between 19 and 24 MeV excitation energy in ^{207}Pb and the possibility of observing the $T_> = \frac{45}{2}$ states in this nucleus is completely dependent upon the concentra-

tion of the single-hole analog strength and the ratio of such cross sections to the physical background arising from the high level density. Finally, the recent calculations of the form factor of such inner hole states^{9,11} using the Lane coupled-channels equations¹² (CC), which have been fairly successful in reproducing the strength of the $T_>$ hole-analog states in heavy nuclei as compared to the usual separation-energy method (SE), could be tested in ^{207}Pb under extreme condition (binding energy of -30 MeV and high isospin number $T_> = \frac{45}{2}$).

In order to study these phenomena in more detail, the reaction $^{208}\text{Pb}(^3\text{He}, \alpha)^{207}\text{Pb}$ was investigated at 70 MeV incident energy using a 50-cm-long delay-line counter backed by a plastic scintillator in the focal plane of the Enge spectro-

Direct Determination of $[(sd)^3]_{5/2, 1/2}(1p^{-2})_{01}$ Component in $^{17}\text{O}(\text{g.s.})$ H. T. Fortune,^(a) J. N. Bishop,^(b) and L. R. Medsker^(c)*Physics Department, University of Pennsylvania, Philadelphia, Pennsylvania 19104*

and

B. H. Wildenthal

Cyclotron Laboratory, Michigan State University, East Lansing, Michigan 48824

(Received 22 May 1978)

Data for the reaction $^{17}\text{O}(^3\text{He}, p)^{16}\text{F}$ to the predominantly five-particle, two-hole $\frac{3}{2}^+$ state at 3.91 MeV in ^{16}F are used to estimate the amount of three-particle, two-hole configuration in $^{17}\text{O}(\text{g.s.})$. The result is 4–6%.

A knowledge of the amount of core excitation in the ground state of ^{17}O is crucial for models¹⁻⁵ that attempt to use experimental electromagnetic- and weak-interaction information for ^{17}O to deduce effective operators or meson-exchange effects. Yet there is no reliable experimental measurement of this quantity. Estimates range from the extreme single-particle value of zero to values as large⁶ as 50%, with a variety of estimates⁷⁻⁹ in between. We report here on a direct determination of the most probable core-excited component.

If the 3.91-MeV $\frac{3}{2}^+$ state¹⁰ of ^{16}F is dominantly five-particle, two-hole (5p-2h) with $T_3=1$, i.e.,

$$[(sd)^5]_{5/2, 1/2}(1p^{-2})_{01},$$

as seems very likely,^{7, 8, 11-13} then the reaction $^{17}\text{O}(^3\text{He}, p)$ to this state provides an excellent method for estimating the 3p-2h core excitation in the $^{17}\text{O}(\text{g.s.})$ that is of the form

$$[(sd)^3]_{5/2, 1/2}(1p^{-2})_{01},$$

where double subscripts denote JT . To make states of good isospin requires

$$5p-2h = \sum_{t_z = \pm 1/2} \left(\frac{1}{2}t_z \mid T_z \mid \frac{1}{2}\frac{1}{2}\right) [(sd)^5]_{5/2, 1/2, t_z}(1p^{-2})_{01, T_z},$$

and

$$3p-2h = \sum_{t_z = \pm 1/2} \left(\frac{1}{2}t_z \mid T_z \mid \frac{1}{2}\frac{1}{2}\right) [(sd)^3]_{5/2, 1/2, t_z}(1p^{-2})_{01, T_z}.$$

Then for $^{17}\text{O}(\text{g.s.})$ of the form $A(1d_{5/2}) + B[(sd)^3]_{5/2, 1/2}(1p^{-2})_{01} + C \times (\text{everything else})$, the amplitude for $^{17}\text{O}(\text{g.s.}) - ^{16}\text{F}(3.91, \frac{3}{2}^+)$ is just B times the amplitude for $[(sd)^3]_{5/2, 1/2} - [(sd)^5]_{5/2, 1/2}$. We take the 3p wave function to be that of the $^{16}\text{F}(\frac{3}{2}^+)$ state at 0.2 MeV excitation and the 5p one to be the $^{21}\text{Ne}(\text{g.s.})$ and use transfer amplitudes for $^{16}\text{F}(\frac{3}{2}^+) - ^{21}\text{Ne}(\text{g.s.})$ from a recent shell-model calculation.¹⁴ These amplitudes are listed in Table I.

The cross section was calculated with the code DWUCK,¹⁵ using standard optical-model parameters.¹⁶ The experimental cross section is related to the one calculated by DWUCK via the expression

$$\sigma_{\text{exp}}(\theta) = \frac{2J_f + 1}{2J_i + 1} NB^2 \sum_{LSJT} D_{sT}^2 b_{sT}^2 (2S+1) C^2 \frac{\sigma_{\text{DW}}(\theta)}{2J+1},$$

TABLE I. Transfer amplitudes (from Ref. 14) for $^{16}\text{F}(\frac{3}{2}^+) - ^{21}\text{Ne}(\text{g.s.})$.

J	T	$(1d_{5/2})^2$	$(1d_{5/2})(2s_{1/2})^2$	$(1d_{5/2})(1d_{3/2})$	$(2s_{1/2})^2$	$(2s_{1/2})(1d_{3/2})^2$	$(1d_{3/2})^2$
1	0	0.0829	0	0.1003	-0.0716	-0.0569	0.0082
2	0	0	-0.0349	-0.0666	0	0.1129	0
2	1	0.8629	-0.4612	-0.2086	0	-0.2279	0.1117
3	0	0.1368	-0.4147	-0.2406	0	0	-0.0144
4	0	0	0	0.1410	0	0	0
4	1	-0.6258	0	-0.0860	0	0	0

^a Signs corrected for input into DWUCK.

Production of $A=6$ and 7 Isotopes in the $\alpha + \alpha$ Reaction

B. G. Glagola, G. J. Mathews,^(*) H. F. Breuer, and V. E. Viola, Jr.

Department of Chemistry and Cyclotron Laboratory, University of Maryland, College Park, Maryland 20742

and

P. G. Roos and A. Nadasen

Department of Physics and Cyclotron Laboratory, University of Maryland, College Park, Maryland 20742

and

Sam M. Austin

Department of Physics and Cyclotron Laboratory, Michigan State University, East Lansing, Michigan 48824

(Received 6 September 1978)

Cross sections have been measured for the production of ${}^6\text{He}$, ${}^6\text{Li}$, ${}^7\text{Li}$, and ${}^7\text{Be}$ in the $\alpha + \alpha$ reaction between 61.5 and 158.2 MeV. The significance of these measurements for theories of lithium nucleosynthesis is discussed.

One of the major deficiencies in our understanding of light-element nucleosynthesis is the apparent inability of single-source model calculations to account for the solar-system abundance ratio of the lithium isotopes, ${}^7\text{Li}/{}^6\text{Li} = 12.5$. In order to provide essential cross-section data for evaluating this problem, we have measured the yields of ${}^6\text{He}$, ${}^6\text{Li}$, ${}^7\text{Li}$, and ${}^7\text{Be}$ in the astrophysically significant $\alpha + \alpha$ reaction from 61.5

to 158.2 MeV. These measurements represent the first systematic determination of the $\alpha(\alpha, {}^6\text{Li})$ and $\alpha(\alpha, {}^6\text{He})$ cross sections over a wide range of energy. In addition, they complete the definition of the excitation functions for $A=6$ and 7 in the $\alpha + \alpha$ reaction, the only major unmeasured reaction necessary for model calculations of Li-Be-B nucleosynthesis.

Along with ${}^2\text{H}$ and the stable isotopes of He,

Comparison of Heavy-Ion-Induced α Transfer and Backward-Angle Elastic Scattering

C. K. Gelbke, T. Awes, and U. E. P. Berg

Cyclotron Laboratory, Michigan State University, East Lansing, Michigan 48824

and

J. Barrette and M. J. LeVine

Department of Physics, Brookhaven National Laboratory, Upton, New York 11973

and

P. Braun-Munzinger

Department of Physics, State University of New York, Stony Brook, New York 11974

(Received 7 July 1978; revised manuscript received 20 October 1978)

Resonancelike structures are observed at backward angles for elastic scattering of $^{12}\text{C} + ^{32}\text{S}$ and for the reaction $^{28}\text{Si}(^{16}\text{O}, ^{12}\text{C})^{32}\text{S}$ which are uncorrelated with the ones seen in the system $^{16}\text{O} + ^{28}\text{Si}$. Analysis of angular distributions indicates that forward α transfer is dominated by partial waves different from those of backward-angle α transfer and elastic scattering in the entrance and exit channels.

Backward-angle excitation functions for the elastic and inelastic scattering of ^{12}C and ^{16}O on ^{28}Si exhibit resonancelike structure.^{1,2} Similar structures have also been seen in the forward-³ as well as backward-angle⁴ excitation functions of the α -transfer reaction $^{24}\text{Mg}(^{16}\text{O}, ^{12}\text{C})^{28}\text{Si}$. Two of the questions arising from previous observations are the following: (i) Are these resonances associated with structure in the compound nucleus, and (ii) are the partial waves responsible for the resonances in the elastic entrance and exit channels simply related to the partial waves dominating transfer reactions?

In this Letter we compare backward-angle elastic excitation functions for two systems, $^{12}\text{C} + ^{32}\text{S}$ and $^{16}\text{O} + ^{28}\text{Si}$, which lead to the same compound nucleus. To study possible connections between structures in large-angle elastic scattering and the recently observed resonance phenomena in forward-angle α transfer,³ we have also measured excitation functions at both forward and backward angles for the reaction $^{28}\text{Si}(^{16}\text{O}, ^{12}\text{C})^{32}\text{S}$. Lack of correlations between the resonances observed in the various channels clearly indicates that they are not produced by common isolated doorway states. Furthermore, angular distributions measured for the reaction $^{28}\text{Si}(^{16}\text{O}, ^{12}\text{C})^{32}\text{S}$ and for the elastic scattering in entrance and exit channels demonstrate that different partial waves dominate forward- and backward-angle cross sections.

The experiment used the ^{12}C , ^{16}O , ^{28}Si , and ^{32}S beams and the quadrupole-triple-dipole magnetic spectrograph of the Brookhaven National Laboratory tandem Van de Graaff facility. The experimental technique has been described in detail.^{1,5} By detecting the outgoing ^{16}O and ^{12}C nuclei, for-

ward-angle cross sections were obtained from the bombardment of 120- $\mu\text{g}/\text{cm}^2$ SiO and 60- $\mu\text{g}/\text{cm}^2$ CdS targets with ^{16}O and ^{12}C ions, while backward angle cross sections were obtained from the bombardment of 100- $\mu\text{g}/\text{cm}^2$ Al_2O_3 and 50- $\mu\text{g}/\text{cm}^2$ C targets with ^{28}Si and ^{32}S ions. The elastic-scattering and forward-angle transfer angular distributions have been measured with an angular resolution of $\Delta\theta_{\text{lab}} \leq 0.9^\circ$. The forward-angle excitation function for the α -transfer reaction has been measured with an angular aperture of $\Delta\theta_{\text{lab}} = 2.9^\circ$, the angle being adjusted to follow the maximum in the angular distribution around $\theta_{\text{c.m.}} = 10^\circ$ (see Fig. 2). All backward-angle excitation functions at $\theta_{\text{c.m.}} = 180^\circ$ have been measured with a solid angle of 8 msr.

The elastic excitation functions at $\theta_{\text{c.m.}} = 180^\circ$ are presented in Fig. 1. The data for the system $^{16}\text{O} + ^{28}\text{Si}$ are from Ref. 1. The system $^{12}\text{C} + ^{32}\text{S}$ exhibits broad structures similar to those observed in the scattering of ^{16}O by ^{28}Si ; however, the average cross section is about one order of magnitude smaller and a strong splitting of the gross structure into fine structure is apparent, similar to the fragmentation observed in the scattering of ^{12}C by ^{28}Si .¹ The striking feature of these data is that there is no obvious correlation between the gross structure observed in the two systems. This result, which is consistent with the observation of Clover *et al.*,⁶ rules out the resonancelike phenomena being generated by a common doorway state in the compound nucleus.

The excitation functions at forward and backward angles for the reaction $^{28}\text{Si}(^{16}\text{O}, ^{12}\text{C})^{32}\text{S}$ are also presented in Fig. 1. Contrary to what has been observed for the system $^{24}\text{Mg}(^{16}\text{O}, ^{12}\text{C})^{28}\text{Si}$,³

Fragmentations of ^{40}Ar at 213 MeV/Nucleon

Y. P. Viyogi,^(a) T. J. M. Symons, P. Doll,^(b) D. E. Greiner, H. H. Heckman, D. L. Hendrie, P. J. Lindstrom, J. Mahoney, D. K. Scott, K. Van Bibber, G. D. Westfall, and H. Wieman
Lawrence Berkeley Laboratory, University of California, Berkeley, California 94720

and

H. J. Crawford and C. McParland
Space Sciences Laboratory, University of California, Berkeley, California 94720

and

C. K. Gelbke
Michigan State University, East Lansing, Michigan 48824
 (Received 11 October 1978)

Energy and isotope distributions were measured for peripheral reactions induced by ^{40}Ar at 213 MeV/nucleon. The data are consistent with the predictions of abrasion-ablation models. The influence of correlations in the nuclear ground state is discussed.

The study of ^{40}Ar -induced reactions at energies below 10 MeV/nucleon has led to important advances in our knowledge of deeply inelastic scattering.¹ At these energies the reaction is believed to proceed by a diffusion mechanism, leading to the emission of fragments from an equilibrated dinuclear system. At much higher energies, it is unlikely that a dinuclear system can ever be formed and there is evidence from studies with light projectiles like ^{16}O that a fast abrasion mechanism² becomes the dominant peripheral process. However, projectile excitation followed by equilibration and decay can also explain many features of the results with ^{16}O .³⁻⁵ Since the characteristic features of heavy-ion reactions at lower energies are much better developed with projectiles like ^{40}Ar , it is likely that a better understanding of the high-energy processes will come from studies on such heavy systems. Here we present the first measurements of energy and isotope distributions in this new energy region with an ^{40}Ar beam at 213 MeV/nucleon.

The experiment used the ^{40}Ar beam of 10^8 particles/sec from the Bevalac to bombard a carbon target of thickness of 400 mg/cm². Projectile

fragments were detected at several laboratory angles in the range 0-4° in a telescope consisting of nine 5-mm-thick silicon detectors, which could stop fragments heavier than nitrogen. The particle identification technique used the algorithm⁶ $(E + \Delta E)^n - E^n \propto TM^{n-1}Z^2$, where T is the thickness of the ΔE detector, M and Z are the mass and charge of the particle, and n was set equal to 1.78. This expression was modified for the case of a multielement detector telescope⁷ to give several identifications. For each event the weighted mean and χ^2 -consistency function were determined. Events arising from reactions in detectors and statistical fluctuations in energy loss were rejected by making cuts on the tail of the χ^2 distribution. The resulting mass spectra had a resolution varying from 0.2 amu for oxygen to 0.5 amu for sulfur.

For isotopes close to the valley of stability, which were produced with high yields, the total cross section was obtained by integrating the angular distributions. For low-yield isotopes far from stability, the cross sections were obtained by adding the yields of all angles and assuming that the angular distributions for these isotopes were the same as for the more-abundant

Incomplete Momentum Transfer in Peripheral Heavy-Ion Collisions at 20 MeV/Nucleon

P. Dyer, T. C. Awes, and C. K. Gelbke

Cyclotron Laboratory, Michigan State University, East Lansing, Michigan 48824

and

B. B. Back, A. Mignerey, and K. L. Wolf

Chemistry Division, Argonne National Laboratory, Argonne, Illinois 60439

and

H. Breuer and V. E. Viola, Jr.

Department of Chemistry, University of Maryland, College Park, Maryland 20742

and

W. G. Meyer

Lawrence Berkeley Laboratory, Berkeley, California 94720

(Received 31 October 1978)

Projectile residues have been studied in coincidence with fragments resulting from fission of the target residue for reactions induced by 315-MeV ^{16}O ions on a ^{238}U target. A kinematical analysis shows that the forward linear momentum transferred to the target nucleus is significantly smaller than that expected for simple transfer reactions, but larger than that expected for pure projectile fragmentation processes.

At energies of only a few MeV per nucleon above the Coulomb barrier, peripheral heavy-ion collisions have been shown to be mainly two-body reactions followed by the subsequent decay of the primary reaction products by particle emission or fission.¹⁻³ At relativistic energies ($E/A \geq 200$ MeV/nucleon), on the other hand, peripheral reactions are largely associated with a projectile fragmentation process in which the target nucleus acts as a mere spectator to which only a small amount of momentum is transferred.⁴ Until now, however, the momentum transfer to the target residue has not been directly measured for heavy-ion reactions above 10 MeV/nucleon. In this Letter we report the first such measurement for the reaction $^{16}\text{O} + ^{238}\text{U}$ at about 20 MeV/nucleon.

The experiment was performed at the 88-in.-cyclotron of the Lawrence Berkeley Laboratory. Targets consisting of 200- $\mu\text{g}/\text{cm}^2$ UF_6 on a 50-

$\mu\text{g}/\text{cm}^2$ carbon backing were bombarded by $^{16}\text{O}^{6+}$ ions of 315 MeV. Projectilelike reaction products were identified with a solid-state ΔE - ΔE - E telescope (27 μm , 70 μm , and 3 mm thicknesses, respectively) at $\theta_{\text{lab}} = 15^\circ$, close to the grazing angle. This telescope allowed the identification of isotopes with a resolution of about 1 amu. Coincident fragments resulting from fission of the target residue were detected by two position-sensitive solid-state detectors, arranged in the geometry shown in Fig. 1. The data were recorded event by event on magnetic tape and analyzed off line. For each event an iterative procedure was used to correct for post-fission neutron evaporation and for pulse-height defects in the fission detectors. Gates were placed on various element numbers and energies of the projectile residues and a kinematical analysis was carried out for each event in order to extract distributions of momentum components parallel to the

A COMPARISON OF 180 MeV π^+ AND π^- SCATTERING FROM ^{24}Mg

C.A. WIEDNER, J.A. NOLEN Jr¹, W. SAATHOFF and R.E. TRIBBLE²

Max-Planck-Institut für Kernphysik, Heidelberg, Fed. Rep. of Germany

J. BOLGER

Institut für Experimentelle Kernphysik, Karlsruhe, Fed. Rep. of Germany

J. ZICHY

Schweizerisches Institut für Nuklearforschung, CH-5234 Villingen, Switzerland

and

K. STRICKER, H. McMANUS and J.A. CARR

Physics Department³, Michigan State University, East Lansing, MI 48824, USA

Received 26 June 1978

Angular distributions for elastic and inelastic scattering of 180 MeV π^+ and π^- beams for ^{24}Mg have been measured. Optical model calculations for the elastic scattering and DWBA calculations for three inelastic transitions are presented.

We have studied elastic and inelastic scattering of 180 MeV π^+ and π^- beams from the self-conjugate nucleus ^{24}Mg . This energy was chosen because recent measurements on ^{12}C at 162 and 226 MeV [1] have shown that the Coulomb induced differences between π^+ and π^- elastic scattering at the first diffraction minimum change sign between these two energies, in agreement with the predictions of Germond and Wilkin [2]. A detailed understanding of such data at the (3, 3) resonance is an essential prerequisite to quantitative interpretation of results such as the ^{40}Ca – ^{48}Ca π^+ and π^- elastic scattering comparisons of ref. [3] at 130 MeV, an energy well below the (3, 3) resonance, where Coulomb induced effects are large even on self-conjugate nuclei.

The present inelastic data on ^{24}Mg show only very small differences between the π^+ and π^- cross sections in agreement with recently published data on a lighter nucleus, ^{12}C , at pion energies in the vicinity of the (3, 3) resonance [1,4]. However, the absolute cross sections for the inelastic transitions seen here are about a factor of two stronger than predicted by a distorted waves collective model calculation. These distorted waves calculations, along with optical model calculations of the elastic scattering and a discussion of the general features of the inelastic spectra are presented below.

The experiment was performed at the Swiss Institute of Nuclear Research (SIN) with the SUSI pion spectrometer. The pion beam line and spectrometer, as well as the multi-wire proportional counters and electronics, are described in references [1,5,6]. Data were recorded in 3° steps over an angular range of 27° to 105° with an energy resolution of about 500 keV FWHM. A 2 mm thick metallic target enriched to 99% in ^{24}Mg was used at angles from 27° to 78° , to which an additional 4 mm thick natural Mg target was added

¹ Permanent address: Cyclotron Laboratory, Michigan State Univ., East Lansing, MI 48824. Research supported in part by the U.S. National Science Foundation.

² A.P. Sloan Fellow (1976–1978). Permanent address: Cyclotron Institute, Texas A & M University, College Station, TX 77843.

³ Research supported in part by the U.S. National Science Foundation.

**CROSS SECTIONS FOR THE QUASIELASTIC $^{112,116,124}\text{Sn}(p, n)$ AND $^{58}\text{Ni}(p, n)$ REACTIONS:
A TEST OF THE FORWARD SCATTERING AMPLITUDE APPROXIMATION [☆]**

S.D. SCHERY

Moody College, Texas A & M University System, Galveston, TX 77550, USA

and

S.M. AUSTIN, A. GALONSKY, L.E. YOUNG and U.E.P. BERG

Cyclotron Laboratory and Physics Department, Michigan State University, East Lansing, MI 48824, USA

Received 3 August 1978

Cross sections for the $^{112,116,124}\text{Sn}(p, n)$ quasielastic reactions have been measured at $E_p = 35.3$ MeV using isotopically mixed targets to provide accurate relative cross sections; $^{58}\text{Ni}(p, n)$ cross sections were measured at 32 MeV. Calculations based on an isospin potential whose imaginary part is calculated in the forward scattering amplitude approximation fit the data substantially better than calculations based on a pure real potential, provided a finite-range correction is included.

The strength and form of the imaginary component of the nucleon-nucleus isospin potential are rather poorly known. This uncertainty is particularly important for (p, n) quasielastic scattering since in the Lane model [1,2] it is the isospin strength that mediates the reaction to the isobaric analogue of the ground state. While the isospin potential is, in principle, complex [3,4], the effects of the imaginary potential are sufficiently small that some investigators have reasonably well reproduced (p, n) data with a purely real potential [5-8]. Others have included an imaginary potential but find that its exact strength and form are substantially uncertain [3,9] and a variety of forms, all of them phenomenological, have been used more or less successfully [8-12].

Although it is fundamentally a high-energy approximation, the forward scattering amplitude (FSA) approximation has been successful in estimating the imaginary potential of the optical model for proton elastic scattering at energies as low as 30 MeV [13]. We report here the results of distorted wave calculations using the FSA approximation for the isospin

component of the imaginary potential and their comparison with (p, n) quasielastic cross sections. When compared to calculations with a real potential alone, inclusion of the FSA imaginary isospin potential results in significantly improved agreement with data. These results indicate that the FSA approximation provides a useful non-phenomenological estimate of the imaginary isospin potential, and adds additional evidence supporting the conclusion that the imaginary isospin potential is important for precise prediction of (p, n) quasielastic data.

To provide a variety of data at a relatively high energy for a test of the FSA approximation, we have measured angular distributions for $^{112,116,124}\text{Sn}(p, n)$ at 35.3 MeV and for $^{58}\text{Ni}(p, n)$ at 32 MeV. Combined with other available data these data span a long isotopic chain, a wide range of $N - Z$, and an energy range up to 45 MeV. Special care, involving use of isotopically mixed targets, was taken to obtain accurate relative cross sections for the Sn isotopes for later use in a determination of neutron density variations in these nuclei. The swinger neutron time-of-flight system at Michigan State University [14] and a large-volume (2700 cm³) neutron detector were used in these measurements. Flight paths of up to 25 m were necessary to resolve

[☆] Research supported in part by the National Science Foundation under Grants Phy78-15064 and Phy78-01684.

SHELL-MODEL PREDICTIONS OF ALPHA-SPECTROSCOPIC FACTORS BETWEEN GROUND STATES OF $16 < A < 40$ NUCLEI

W. CHUNG

IKP, KFA Jülich GmbH, D-5170 Jülich, W. Germany

J. van HIENEN¹ and B.H. WILDENTHAL

Cyclotron Laboratory², Michigan State University, E. Lansing, MI 48824, USA

and

C.L. BENNETT

NSRL, University of Rochester, Rochester, NY 14627, USA

Received 25 September 1978

Shell-model wave functions in the complete $0d_{5/2}-1s_{1/2}-0d_{3/2}$ basis space are used to calculate the alpha-spectroscopic factors for ground-state to ground-state transitions in the $16 < A < 40$ region. The results are compared to various families of experimental data, and to predictions of the SU(3) approximation.

The systematics of the spectroscopic strength for alpha-like cluster transfer on targets in the sd-shell have been investigated experimentally with various reactions [1-5]. Comprehensive theoretical interpretations of these systematics are difficult because, among other reasons, the increments of four nucleons between target and final systems require that comparably and mutually consistent calculations must be carried out over a large range of masses. To date, theoretical interpretations of the alpha transfer strengths have employed the SU(3) approximation [6] for the wave functions and this in turn has limited considerations at best to the model of the lower half of the shell, for which SU(3) provides an effective description of many states. In the present note we take advantage of a recent calculation [7] in which wave functions for all ground states of sd-shell nuclei have been obtained in the $j-j$ representation under the assumptions of a uniform model

space, the complete set of basis vectors formed with the $0d_{5/2}$, $1s_{1/2}$, and $0d_{3/2}$ orbits, and one or the other of two similar hamiltonians. These hamiltonians were empirically adjusted to fit energy-level data in, alternatively, the lower and upper halves of the shell and they yield similar results for nuclei in the middle of the shell. We have evaluated the four-nucleon overlaps [8] between these ground state wave functions and calculated alpha-spectroscopic amplitudes defined [9] as a sum of products of three factors:

$$S^{1/2} = \left(\frac{A}{A-4} \right)^{N+L/2} \sum_{\Gamma} \langle \Psi_A \| \chi_{\alpha}^{\Gamma} \| \Psi_{A-4} \rangle \times \langle \Phi_{\text{int}}(\xi_{\alpha}) \Phi_{\text{NL}}(R_{\alpha}) | \Psi_{\text{SM}}^{\Gamma}(\xi_{\alpha}) \rangle. \quad (1)$$

The first factor is the coefficient resulting from a coordinate transformation which, within the harmonic oscillator framework, transforms the shell-model wave functions from a representation in a fixed coordinate system to a representation in systems of relative and center-of-mass motion. The second factor is a reduced matrix element of the four-nucleon creation operator with quantum numbers Γ calculated from the shell-

¹ Present address: Vrije Universiteit, Amsterdam, The Netherlands.

² This material is based upon work supported by the National Science Foundation under Grant No. Phy 78-01684.

ELECTROEXCITATION AND THE DETERMINATION OF THE K-BAND STRUCTURE IN ^{24}Mg *

H. ZAREK, S. YEN, B.O. PICH and T.E. DRAKE

Department of Physics, University of Toronto, Ontario, Canada M5S 1A7

C.F. WILLIAMSON, S. KOWALSKI and C.P. SARGENT

Department of Physics and Laboratory for Nuclear Science, Massachusetts Institute of Technology, Cambridge, MA 02139, USA

W. CHUNG and B.H. WILDENTHAL

Cyclotron Laboratory and Physics Department, Michigan State University, East Lansing, MI 48823, USA

and

M. HARVEY and H.C. LEE

Atomic Energy of Canada Limited, Chalk River Nuclear Laboratories, Chalk River, Ontario, Canada K0J 1J0

Received 26 September 1978

The high-resolution electron scattering facility at the MIT-Bates accelerator was used to resolve the 4_1^+ 4.12 MeV and 2_2^+ 4.24 MeV levels in ^{24}Mg . The respective E2 and E4 Coulomb form factors were measured and compared to form factors calculated theoretically; the 4_1^+ form factor exhibits a momentum-transfer dependence which strongly suggests that K is a good quantum number in ^{24}Mg .

In this letter we report the results of a recent (e, e') experiment on ^{24}Mg and, by comparison of the strengths and shapes of the form factors with those from a projected Hartree-Fock (PHF) calculation, surmise that the lowest $J^\pi = 2^+$ and 4^+ states must belong to almost pure $K = 0$ and $K = 2$ bands. This conclusion is possible because we have, for the first time, managed to resolve the excitations to the 4_1^+ 4.12 MeV and the 2_2^+ 4.24 MeV levels. A further comparison with a renormalised spherical shell model (SM) calculation yields insight into the use of effective operators. Hence even though the shell model appears to successfully account for $B(E\lambda)$ values of low-lying 2^+ and 4^+ states in ^{24}Mg , the new electron scattering data show that this description is very far from complete.

* Research supported in part by the National Research Council of Canada and in part by the U.S. Energy Research and Development Administration under Contract No. E(11-1) 3069.

The present (e, e') experiments were performed with the high-resolution electron scattering facility at the MIT-Bates accelerator [1]. A portion of a typical inelastically-scattered electron spectrum is shown in fig. 1, taken at a spectrometer angle of 90.0° and an incident electron energy of 218.1 MeV. Here the 4.12 and 4.24 MeV levels are clearly resolved. A target of thickness $25.2 \pm 0.1 \text{ mg/cm}^2$, area $4.5 \text{ cm} \times 4.0 \text{ cm}$, and isotopic purity of 99.4% ^{24}Mg was used. The measurements were made relative to the observed elastic peak, and to the inelastic peaks of the 2_1^+ state at 1.37 MeV and the 4_2^+ state at 6.01 MeV excitation in ^{24}Mg , the Coulomb form factors of which have been previously measured [2-4]. Normalization was also made relative to the elastic peak of ^{12}C , observed with a graphite target.

The form factor for inelastic electron scattering to an isolated level is given in plane-wave Born approximation (PWBA) by [5]

DAMPING OF SINGLE-PARTICLE STATES AND GIANT RESONANCES IN ^{208}Pb G.F. BERTSCH¹*Cyclotron Laboratory, Michigan State University, East Lansing, MI 48824, USA*

and

P.F. BORTIGNON², R.A. BROGLIA and C.H. DASSO³*The Niels Bohr Institute, University of Copenhagen, DK-2100 Copenhagen Ø, Denmark*

Received 17 October 1978

The damping width of single-particle states and of giant resonances is estimated in ^{208}Pb , based on the excitation of surface modes and $T = 1$ pairs. The damping is dominated by the collectivity of the surface modes, with the pairing modes playing a weaker role. For both the single-particle states and giant resonances, the predicted damping is somewhat small. This could be due to the neglect of $T = 0$ particle-particle correlations or to the neglect of the volume modes. The damping for the giant resonances is reduced by the coherence between particle and hole.

A systematic description of the low-lying nuclear spectrum can be achieved for single- and doubly-closed shell nuclei in terms of surface and pairing vibrations, together with single nucleon degrees of freedom. This model has been very successful for nuclei in the neighborhood of ^{208}Pb , (cf. e.g. ref. [1]). The dominance of the surface degrees of freedom in the nuclear vibrations has been justified microscopically with the self-consistent RPA model [2]. A perturbation expansion can be constructed which explicitly displays these degrees of freedom and is in principle exact. This expansion, which we call Nuclear Field Theory (NFT) allows boson and fermion interactions through the two-body residual nuclear interaction and through particle-vibration couplings. The expansion parameter in the NFT approach to the nuclear many-body problem is $1/\Omega$, Ω being the effective degeneracy of the valence shells.

In the present paper we apply the NFT to the calcu-

lation of the width of single-particle states and of giant isoscalar resonances in ^{208}Pb . There is extensive literature on the theory of widths of single-particle states [3-9] and of giant vibrations [10-17]. However, these works do not treat the single-particle states and the giant vibrations together, and so do not reach firm conclusions on the validity of the models applied. By focussing on one quantity alone, the damping width, we shall show that existing theory accounts quite well for the relative magnitude of damping in single-particle states and in vibrations, but falls short on absolute magnitudes.

In the NFT, the lowest-order contributions to the width of a single-particle state, Γ_p , are given by the imaginary parts of the self-energy graphs shown in fig. 1A-C,

$$\Gamma_p = 2 [\text{Im}(\Sigma_A - \frac{1}{2}\Sigma_C) + \text{Im}\Sigma_B]. \quad (1)$$

In graphs 1A and 1B, a particle is damped by bouncing inelastically off the nuclear surface, exciting a particle-hole or a pairing vibration. Graph 1C, which distinguishes the lowest-order NFT from other particle-vibration models, is necessary to correct for the miscounting of the exchange interaction in graph 1A [18]. To order $1/\Omega$ there is no corresponding correction to Σ_B . However, there is a graph of order $1/\Omega^2$ which is equivalent

¹ Supported by the National Science Foundation, Grant No. PHY-76-20097 A01.

² Present address: Istituto di Fisica Galileo Galilei, Padova, Italy; INFN Sez. Padova, Italy.

³ Present address: Institut für Kernphysik, Heidelberg, West Germany.

MONOPOLE EXCITATIONS IN ^4He , ^{12}C AND ^{24}Mg IN A COLLECTIVE MODEL DESCRIPTION

H.P. MORSCH

*Cyclotron Laboratory, Michigan State University, East Lansing, MI 48824, USA, and
Kernfysisch Versneller Instituut der Rijksuniversiteit, Groningen, The Netherlands*¹

and

P. DECOWSKI

*Cyclotron Laboratory, Michigan State University, East Lansing, MI 48824, USA, and
Department of Nuclear Physics, University of Warsaw, Poland*

Received 29 December 1977

Revised manuscript received 27 September 1978

Transition densities for monopole excitations have been derived from a simple collective model. Two different monopole modes are obtained, a surface vibration and a density mode which involves a change of the central nuclear density. The low lying monopole transition in ^{24}Mg is well described by a surface vibration. However, for the light systems ^4He and ^{12}C surface and density effects cannot be separated.

Shape transitions (without transfer of angular momentum) are directly related to compressional features of the nucleus. Apart from recent evidence for the compressional mode in heavy nuclei [1] this type of excitation has been studied experimentally only for light nuclear systems in electron [2,3] and hadron scattering [4-6]. The microscopic interpretation of these transitions is difficult because it depends sensitively on the amount of n -particle- n -hole configuration mixing in ground and excited 0^+ state (see ref. [4,5]). In the present letter we discuss a simple macroscopic model in which the experimental data are well described. Because of its large simplicity this model yields direct insight into the mechanism of these excitations.

A Taylor expansion of the nuclear density is used to derive collective monopole transition densities. This model is similar to that used by Satchler in a potential model approach [7]. The parameters x_i of the ground state density are treated as dynamical parameters, so the transition density $\Delta\rho(r)$ can be expressed by derivatives of the ground state density $\rho(r)$:

$$\Delta\rho(r) = \sum_{i=1}^n \delta x_i \frac{\partial\rho(r)}{\partial x_i} + \text{higher order terms (h.o.)}. \quad (1)$$

The orthogonality of initial and final state gives rise to the constraint $\int \Delta\rho(r) d\tau = 0$, this yields a relation between the different δx_i . Thus, eq. (1) represents a system of $(n-1)$ basis states representing $(n-1)$ different monopole excitation modes. The higher order terms of the form

$$\sum_{i,j} \delta x_i \delta x_j \frac{\partial^2\rho(r)}{\partial x_i \partial x_j} + \dots,$$

are important for the large density changes in the light nuclei in question and give rise to anharmonic effects.

We discuss two different ground state shapes, a Gaussian $\rho(r) = \rho_0 \exp(-r^2/\gamma^2)$ and a Woods-Saxon density $\rho(r) = \rho_0(1 + \exp(r-R/a))^{-1}$. For the Gaussian shape we obtain only one transition density

$$\Delta\rho(r) = \delta\rho_0 \frac{\partial\rho(r)}{\partial\rho_0} + \delta\gamma \frac{\partial\rho(r)}{\partial\gamma} + (\text{h.o.}), \quad (2)$$

whereas the Woods-Saxon form gives rise to two different monopole modes with transition densities

¹ Present address: Institut für Kernphysik, Kernforschungsanlage Jülich, Jülich, Germany.

$^{21}\text{Ne}(^3\text{He}, p)^{23}\text{Na}$ reaction

H. T. Fortune,* J. R. Powers,† and R. Middleton
 Physics Department, University of Pennsylvania, Philadelphia, Pennsylvania 19104

H. Nann† and B. H. Wildenthal
 Cyclotron Laboratory, Michigan State University, East Lansing, Michigan 48823
 (Received 24 March 1978)

The reaction $^{21}\text{Ne}(^3\text{He}, p)^{23}\text{Na}$ has been investigated at a bombarding energy of 18.0 MeV, using enriched ^{21}Ne gas contained in a rotating gas cell. Angular distributions for the positive-parity states have been analyzed with the distorted-wave Born approximation, using transfer amplitudes from an $(sd)^7$ shell-model calculation. Agreement with experiment is good. Tentative correspondences are suggested for all experimental and theoretical levels below 6 MeV excitation. Low-lying negative-parity states are very weakly populated.

NUCLEAR REACTIONS $^{21}\text{Ne}(^3\text{He}, p)$, $E = 18.0$ MeV; measured $\sigma(E_p, \theta)$. ^{23}Na deduced levels L, J, π . DWBA analysis with shell-model wave functions. Enriched gas target.

I. INTRODUCTION

The most severe critique of existing nuclear shell-model theory is its ability to predict correctly observables for nuclei in the middle of a shell.

A rather sensitive test of the wave functions of the initial and final states can be provided by the comparison of experimental two-nucleon transfer differential cross sections with microscopic distorted-wave Born approximation (DWBA) calculations based on matrix elements of the coupled two-particle creation (or annihilation) operator.

In the case of the reaction under study here $^{21}\text{Ne}(^3\text{He}, p)^{23}\text{Na}$, most of the levels in the final nucleus ^{23}Na below 6 MeV of excitation have known¹ spin and parity. All of them that are known to have even parity can be identified with states predicted in an $(sd)^7$ shell-model calculation.² Except for a $K^\pi = \frac{7}{2}^+$ rotational band that is predicted, but not observed, the agreement between calculated and measured energies is very good, as depicted in Fig. 1.

Spectroscopic amplitudes calculated from the wave functions of Ref. 2 were used with DWBA calculations to predict the shapes and relative differential cross sections of transitions to even parity states in ^{23}Na . The ability to reproduce the shape of the experimental angular distributions and the consistency of the ratio of the measured and calculated cross sections then give a measure of the goodness of the theoretical wave functions.

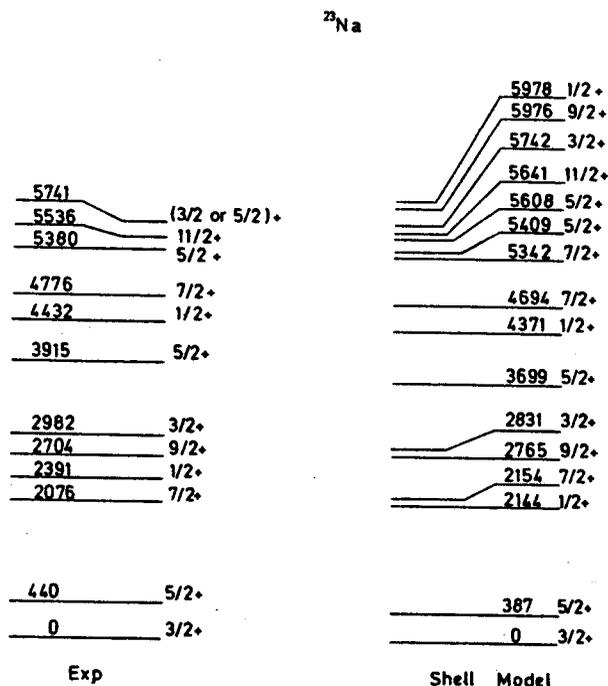


FIG. 1. Experimental levels of ^{23}Na (left, Ref. 1) known to have positive parity prior to present work compared with energies calculated in an $(sd)^7$ basis (right, Ref. 2). Only levels below 6 MeV are included.

II. EXPERIMENTAL PROCEDURE AND RESULTS

The experiment was performed with an 18-MeV ^3He beam from the University of Pennsylvania tan-

Inelastic scattering of 40 MeV protons from ^{24}Mg . II. Microscopic calculations for positive parity states

B. Zwieglinski,* G. M. Crawley, W. Chung,** H. Nann,[†] and J. A. Nolen, Jr.

Cyclotron Laboratory, Michigan State University, East Lansing, Michigan 48824

(Received 11 April 1978)

Proton inelastic scattering data at 40 MeV bombarding energy are compared to microscopic distorted-wave Born-approximation calculations for positive parity states in ^{24}Mg utilizing shell-model wave functions spanning the full $2s1d$ shell basis. Both empirical forces and forces derived from free nucleon-nucleon potentials are used in the calculations. Except for four transitions for which strong coupling effects are evident, the agreement between theory and experiment is quite good. Enhancement factors extracted for the natural parity transitions are consistent with the effective charges obtained from electromagnetic transition rates. Levels corresponding to the giant $M1$ resonance in ^{24}Mg have been resolved in the present experiment. The fact that the renormalization factor between theory and experiment is close to unity for the 10.713 MeV 1^+ ; $T = 1$ state indicates that little or no renormalization of the two-body force is necessary for this inelastic transition. It is argued that little renormalization is also involved for magnetic-type inelastic transitions of multi polarities higher than $M1$.

NUCLEAR REACTIONS $^{24}\text{Mg}(p, p')$ at 40 MeV to positive parity states. Microscopic DWBA analysis with the full $2s1d$ basis wave functions. Deduced collective enhancement factors.

I. INTRODUCTION

Due to recent progress in nuclear shell-model calculational techniques,¹ the wave functions of the $2s1d$ -shell nuclei calculated in the complete $2s1d$ -shell basis are presently available.² The predictions of these calculations have been compared with the traditional spectroscopic observables such as static and transition electromagnetic moments, beta decay log ft values and single nucleon spectroscopic factors. Another test of these wave functions is in the calculation of the nucleon inelastic scattering cross sections using a microscopic reaction theory. Sophisticated microscopic calculations of inelastic proton scattering are now possible, including finite range effects and exchange contributions and allowing for tensor and spin-orbit terms in the effective two-body interaction. In previous work in this mass region, calculations have been restricted to nuclei possessing fairly simple structure. They proved quite successful in interpreting the transitions to the members of the particle-hole multiplets in the closed-shell ^{16}O (Ref. 3) and ^{40}Ca (Refs. 4,5) nuclei. Some transitions in nuclei with a few nucleons beyond the closed ^{16}O core have been also analyzed assuming simple shell-model⁶ and Hartree-Fock⁷ wave functions.

Nuclei near the middle of the sd -shell like ^{24}Mg provide a particularly severe test of the shell-model wave functions. Therefore the main purpose of the present work was to determine whether the wave functions of Chung and Wildenthal² calculated in the full sd -shell basis can account for the $^{24}\text{Mg}(p, p')$ cross sections at $E_p = 40$ MeV. A second purpose was to investigate core polarization effects. The concept of the core polarization has been introduced⁸ in order to account for the participation of configurations from outside of the model space in the transitions. Core contributions are taken into account by renormalizing the operators acting within the model space. This is accomplished by introducing effective charges into the electromagnetic operators and enhancement factors into the effective nucleon-nucleon force^{9,10} used to calculate the inelastic cross sections. The cases most thoroughly studied at present are the core polarization effects involved in the transitions to the low-

lying collective 2^+ and 3^- states (even-even target nuclei only are considered throughout the present paper). Core contributions are constructively coherent with the contributions of the valence particles for these electric-type inelastic scattering transitions, resulting in cross sections enhanced over the shell-model estimates.

Particular attention has been paid in the present work to extraction of the cross sections for the transitions to the unnatural parity states. These transitions involving the matrix elements of the spin operator will be termed magnetic-type following the terminology introduced in Ref. 11. These magnetic-type transitions have been much less studied in the past than electric-type transitions. It is of interest to establish whether the proportionality of the excitation strengths previously observed¹² between the electromagnetic and the isoscalar electric-type inelastic excitations holds also for the magnetic-type transitions. This is expected on the basis of the similarity of the matrix elements involved in their description.¹¹ For example, bare-nucleon g -factors in the magnetic moment operator and the full sd -shell basis wave functions are sufficient to reproduce the magnetic moments of the $A = 17-25$ nuclei.¹³ One of the purposes of the present work is to determine whether the bare two-body force suffices to reproduce the l^+ , $T = 1$ cross sections seen in the present data.

For the analogs of the giant $M1$ resonance in ^{28}Si , an approximate proportionality of the charge-exchange (t, He) reaction cross sections to the reduced $M1$ excitation strengths has been reported.¹⁴ However, the conclusions from the study of the l^+ , $T = 1$ states with nucleon induced inelastic scattering and charge-exchange reactions may be more convincing, since contributions from two-step stripping and pick-up processes are known to be important for reactions with mass-3 projectiles.

The angular distributions for the inelastic scattering of 40 MeV protons from the positive parity states of ^{24}Mg in the excitation energy range up to 11 MeV are discussed in the present work. The high resolution achieved with the MSU cyclotron and the Enge split-pole spectrograph permitted the extraction of cross sections for many more states than previously observed in inelastic scattering on ^{24}Mg . The details of the experimental method and the

Mass measurement of proton-rich, medium-weight nuclei by the ($^3\text{He}, ^6\text{He}$) reaction

R. C. Pardo, E. Kashy, W. Benenson, and L. W. Robinson
Cyclotron Laboratory, Michigan State University, East Lansing, Michigan 48824
 (Received 4 May 1978)

The ($^3\text{He}, ^6\text{He}$) reaction at 70 MeV on ^{70}Ge , ^{90}Zr , ^{106}Cd , ^{112}Sn , and ^{144}Sm has been used to study the proton-rich nuclei ^{67}Ge , ^{87}Zr , ^{103}Cd , ^{109}Sn , and ^{141}Sm . The observed ground state mass excesses have been determined to be -62.65 ± 0.03 , -79.344 ± 0.009 , -80.620 ± 0.018 , -82.634 ± 0.011 , -75.933 ± 0.016 MeV, respectively. Excited states observed in these reactions are also reported. The cross sections for the ($^3\text{He}, ^6\text{He}$) reaction decrease with increasing A but not as dramatically as has been observed with the ($^3\text{He}, ^7\text{Be}$) reaction.

NUCLEAR REACTIONS ^{70}Ge , ^{90}Zr , ^{106}Cd , ^{112}Sn , ^{144}Sm ($^3\text{He}, ^6\text{He}$) ^{67}Ge , ^{87}Zr , ^{103}Cd , ^{109}Sn , ^{141}Sm ; $E = 70$ MeV; measured reaction Q values, deduced mass excesses, excitation energies.

I. INTRODUCTION

The masses of medium-weight, proton-rich nuclei have been determined mainly by beta decay end-point measurements. For a nucleus far-from-stability the mass excess (M.E.) is obtained by combining successive beta end-point measurements until one reaches either a stable nucleus or a nucleus whose mass excess is known from a Q value determination in a charged particle reaction. The determination of the mass excesses of even a few nuclei far-from-stability via charged particle reactions is highly desirable because accurate determinations can be expected to improve the binding energy information in an entire region surrounding these nuclei.

The ($^3\text{He}, ^6\text{He}$) reaction has been a powerful method for studying proton-rich nuclei in the mass region up to zinc. It has not been previously applied to heavier nuclei, due in part to the assumption that the already extremely small cross section would become even smaller, much as had been observed in the ($^3\text{He}, ^7\text{Be}$) reaction.¹

In this paper we report the observation of the ($^3\text{He}, ^6\text{He}$) reaction on targets of ^{70}Ge , ^{90}Zr , ^{106}Cd , ^{112}Sn , and ^{144}Sm . The measured Q -values yield new determinations of mass excesses for ^{67}Ge , ^{87}Zr , ^{103}Cd , ^{109}Sn , and ^{141}Sm . In addition, several excited states were identified in each nucleus. We also report the cross sections observed and discuss the global trends of cross-section for the ($^3\text{He}, ^6\text{He}$) reaction.

II. EXPERIMENTAL METHOD

The Michigan State University cyclotron provided 70 MeV ^3He beams with typical intensities of $1 \mu\text{A}$ on target. The reaction products were detected in the focal plane of an Enge split-pole magnetic spectrograph using a two-wire charge-division gas proportional counter for position and ΔE information in a manner previously described.² Time-of-flight and light output information were provided by a plastic scintillator backing the proportional counters. The ^6He reaction products were identified using the resulting ΔE , light output, and TOF information. The data were event recorded using a PDP 11/45 computer for final off-line sorting.

The targets used in this study are listed in Table I. The target thicknesses were measured using α particles of

8.785 MeV energy from sources produced by ^{228}Th decay products. The errors in the measured Q values due to the uncertainties in the target thickness were less than 6 keV except for ^{106}Cd , where the nonuniformity of the target contributed 12 keV. Either the $^{60}\text{Ni}(^3\text{He}, ^6\text{He})^{59}\text{Ni}$ ($Q = -11.054 \pm 0.004$ MeV) or the $^{62}\text{Ni}(^3\text{He}, ^6\text{He})^{59}\text{Ni}$ ($Q = -8.255 \pm 0.002$ MeV) reactions were chosen as the calibration reactions because they have almost the same Q value as the reactions of interest. This made it unnecessary to change the magnetic field of the spectrograph, and eliminated a major source of error in the Q value determination.

The data were acquired in a sequence consisting of calibration-measurement-calibration. The requirement that the calibrations before and after the measurement agree insured against errors due to field change, detector malfunction, or other similar problems. Measurements

TABLE I. Targets

Target	% Enrichment	Thickness ($\mu\text{g}/\text{cm}^2$) ^{a)}	
		Target	^{12}C Backing
^{70}Ge	84.62	310	20
^{90}Zr	98.66	245	
^{106}Cd	82.90	1100	
^{112}Sn	80.04	850	
^{144}Sm	95.1	645	25
^{60}Ni	99.79	258	
^{62}Ni	98.83	239	

^{a)} Unless specified, all targets were self-supporting foils.

Heavy ion collisions at intermediate energy

G. Bertsch

Physics Department, Michigan State University, East Lansing, Michigan 48824

A. A. Amsden

Theoretical Division, Los Alamos Scientific Laboratory, Los Alamos, New Mexico 87545

(Received 24 March 1978)

Two types of measurement are proposed for the analysis of heavy ion collisions in the range of energy of 20–200 MeV/A. First, measurement of the longitudinal component of the kinetic energy of the collision products characterizes the impact parameter of the collision. The distribution in this quantity allows the dissipation in the theoretical models to be determined. A second kind of measurement is that of the coefficients of a spherical harmonic expansion of the angular distribution of the products. Besides giving independent information on the impact parameter and reaction dynamics, measurement of these coefficients offers the possibility of measuring the stiffness of the equation of state of nuclear matter. These ideas are explored in the context of a hydrodynamic model for the collision. In the purely hydrodynamic model there is a large measurable asymmetry in the angular distribution, but the dependence on the equation of state is small.

[NUCLEAR REACTIONS Heavy ion collisions. Energy loss and angular distributions discussed and related to dissipation mechanism, equation of state. Hydrodynamic calculations.]

INTRODUCTION

An important motivation for measuring heavy ion collision cross sections at intermediate energy is to study nuclear matter at high density. In particular, we would like to know whether there are any unusual phenomena such as phase transitions, associated with high density nuclear matter. The quantitative goal is to infer information about the nuclear equation of state from the experimental observables.

To date, no clear dependence of experimental observables on the fundamental properties of nuclear matter has been demonstrated. The type of experiment carried out most extensively is the measurement of the energy- and angle-differential cross section for various kinds of collision products,¹ summing over all final states. The theoretical predictions for these measurements have been found to be remarkably insensitive to the theoretical model.² The basic problem is that an inclusive cross section measurement averages over the impact parameter of the collisions, and much information is lost. We propose two measurements of energy and angular distribution that involve all of the collision products. While much more difficult to interpret experimentally, we will show below that these quantities can be readily interpreted theoretically.

ENERGY

We propose that the total c.m. kinetic energy in the longitudinal direction be measured for col-

lisions between the equal mass target and the projectile. Nonrelativistically, this can be defined as

$$E_{\parallel} = \sum_i \frac{p_{\parallel}(i)^2}{2m_i}, \quad (1)$$

where the sum is over all collision products, and $p_{\parallel}(i)$ is the momentum of the i th particle along the beam direction. The experimental measurement will give a probability distribution in E_{\parallel} , which we call dN/dE_{\parallel} . The value of E_{\parallel} for a particular collision will correlate with the impact parameter; the point at which dN/dE_{\parallel} goes to zero will correspond to head-on collisions. The value of E_{\parallel} at the small impact parameters is quite dependent on the model of the collision, the variation depending on how quickly the coherent motion of the two heavy ions coming together is converted to thermal energy by nucleon-nucleon collisions.

One extreme is the hydrodynamic model, in which the pressure tensor is assumed to be isotropic. In this situation, the nuclear matter is sprayed out in the transverse direction when there is a head-on collision. Thus E_{\parallel} will be quite small for these collisions. We illustrate this with numerical 3-D hydrodynamic calculations. The calculation scheme and other results are described in Ref. 3. We consider collisions of mass 40 nuclei, at energies of 100 MeV/A (lab) and 400 MeV/A (lab), using the same equation of state as in Ref. 3. In Fig. 1 we show the longitudinal energy fraction as a function of impact parameter. We see that there is not a significant difference between the two energies. In Fig. 2 we plot the

Configuration of $^{19}\text{Ne}(4.033, 3/2^+)$

H. T. Fortune*

Physics Department, University of Pennsylvania, Philadelphia, Pennsylvania 19104

H. Nann† and B. H. Wildenthal

Cyclotron Laboratory, Michigan State University, East Lansing, Michigan 48824

(Received 27 April 1978)

Data for the $^{21}\text{Ne}(p,t)$ reaction to the $3/2^+$ state at 4.03 MeV excitation in ^{19}Ne are consistent, both in angular distribution shape and cross-section magnitude, with calculations that assume a dominant 5p-2h configuration for this state.

[NUCLEAR REACTIONS $^{21}\text{Ne}(p,t)$, $E=40$ MeV; measured $\sigma(E_i, \theta)$. ^{19}Ne levels]
deduced configuration. DWBA with microscopic wave functions.

We have used the $^{21}\text{Ne}(p,t)$ reaction in an attempt to determine the configuration of the level¹ at 4.033 MeV in ^{19}Ne . This state has a $J^\pi = (\frac{3}{2}, \frac{5}{2})^+$ assignment² from a weak $l=2$ angular distribution in $^{20}\text{Ne}(\text{He}, \alpha)$. It is populated with an apparent $L=0$ angular distribution³ in $^{21}\text{Ne}(p,t)$, which would imply $J^\pi = \frac{3}{2}^+$. The mirror state at 3.907 MeV in ^{19}F has a firm $J = \frac{3}{2}$ assignment,⁴ and has been taken to have positive parity from mirror correspondence.

The configuration of these two levels has long been a perplexing problem. Weak-coupling calculations^{5,6} suggest a five-particle-two-hole (5p-2h) and/or 7p-4h structure. A Nilsson model calculation, on the other hand, suggests⁷ the state to be the band head of a $K^\pi = \frac{3}{2}^+$ 3p band. Rogers, in a critical review⁸ of all the data available at the time, concluded that the 3907 level of ^{19}F was an "intruder state", not of $(sd)^3$ character, and that the $(sd)^3$ Nilsson interpretation⁷ was very unlikely because of several definite shortcomings.

The state is very weak in a variety of particle transfer reactions,^{2,9-16} consistent with the intruder interpretation. In fact, in all of the reactions studied, it is strong only in (p,t) , making this a good reaction with which to investigate its configuration. Thus, we have used this reaction to obtain a quantitative estimate of the predominant wave-function components of this state.

The experiment was performed with a 40 MeV proton beam from the Michigan State University cyclotron. Tritons were momentum analyzed in a split-pole spectrograph and detected in a position-sensitive detector. The target was neon gas (enriched in ^{21}Ne) contained in a closed gas cell. Data were obtained at twelve angles between 8° and 50° (lab).

In order to obtain an internal absolute normalization for the reaction calculations, data were

also analyzed for the strong $\frac{5}{2}^+$ state¹ at 238 keV excitation. Angular distributions for the two states are displayed in Figs. 1 and 2. Theoretical angular distributions were calculated with the microscopic two-nucleon transfer option of the code DWUCK,¹⁷ using two-nucleon transfer amplitudes from shell-model calculations^{18,19} and standard

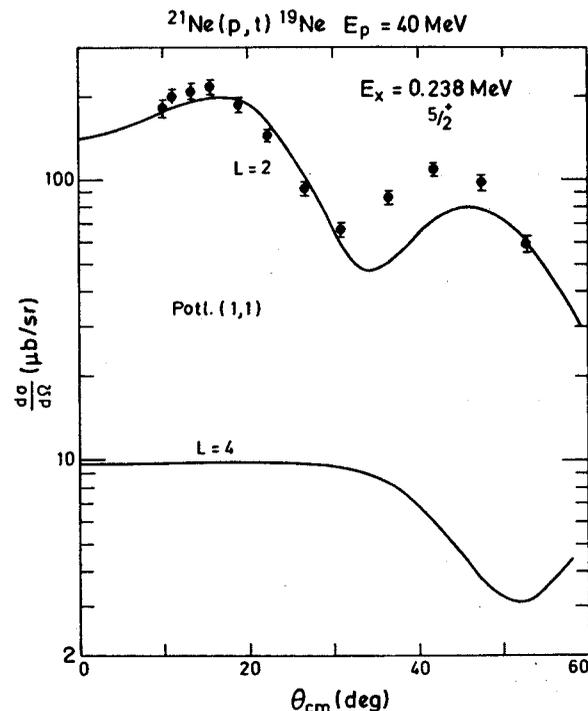


FIG. 1. Experimental angular distribution for the reaction $^{21}\text{Ne}(p,t)^{19}\text{Ne}$ populating the $\frac{5}{2}^+$ state at $E_x = 0.238$ MeV. Curves are results of DWBA calculations using shell-model transfer amplitudes. The extracted normalization factor is $N=142$.

Energy levels in ^{57}Ni from a study of the $^{59}\text{Ni}(p, t)^{57}\text{Ni}$ reaction

H. Nann* and A. Saha†

Cyclotron Laboratory and Department of Physics, Michigan State University, East Lansing, Michigan 48224

S. Raman

Physics Division, Oak Ridge National Laboratory, Oak Ridge, Tennessee 37830

(Received 30 May 1978)

Energy levels in ^{57}Ni up to an excitation energy of 9 MeV have been studied by the $^{59}\text{Ni}(p, t)^{57}\text{Ni}$ reaction at 40 MeV bombarding energy. An energy resolution of 10–15 keV for the triton groups permitted the identification of about 50 new levels. Unambiguous spin and parity assignments of $3/2^-$ are made to the levels at 0.00, 3.01, 4.92, and 5.19 MeV on the basis of an $L = 0$ admixture in the angular distributions. Values of the orbital angular momentum L transferred to several states have been deduced.

NUCLEAR REACTIONS $^{59}\text{Ni}(p, t)$, $E = 40$ MeV; measured $\sigma(\theta)$. ^{57}Ni deduced levels, L , J^π . DWBA analysis. Enriched target.

I. INTRODUCTION

In a simple shell-model picture, the low-lying states of ^{57}Ni can be described as arising from a neutron in the $2p_{3/2}$, $1f_{5/2}$ or $2p_{1/2}$ orbitals outside the doubly-closed nucleus ^{56}Ni even though experimentally these single-particle aspects cannot be fully explored due to the lack of suitable targets. The level structure of ^{57}Ni has been investigated with single-neutron pickup reactions on $^{58}\text{Ni}^{1-7}$ and with the $^{54}\text{Fe}(\alpha, n\gamma)$ reaction.^{8,9} Energy levels up to 8.8 MeV have been determined via the $^{58}\text{Ni}(p, d)^{1,2}$, $^{58}\text{Ni}(d, t)^{3,4}$, and $^{58}\text{Ni}(^3\text{He}, \alpha)^{5-7}$ reactions, and values of the single-neutron angular momentum transfer, l_n , have been deduced for a few transitions. Measurements of the vector analyzing power³ and particle-gamma angular correlations⁷ have yielded spin and parity (J^π) assignments for some low-lying levels. The $^{54}\text{Fe}(\alpha, n\gamma)^{57}\text{Ni}$ reaction^{8,9} has been used to determine the energies, decay modes and lifetimes of the first five excited states of ^{57}Ni .

The present investigation of the (p, t) reaction on radioactive ^{59}Ni was undertaken with the aim of extending the existing experimental information about ^{57}Ni . Angular distributions were obtained for approximately 35 out of a total of 77 levels up to an excitation energy of 9 MeV.

II. EXPERIMENTAL PROCEDURE

The present experiment was performed with a 40 MeV proton beam from the Michigan State University Cyclotron. The triton groups were momentum analyzed in a Enge split-pole spectrograph and detected in the focal plane by a position-sensitive proportional counter with delay-line readout, backed by a plastic scintillator. This detector system provided excellent spatial resolution and particle identification. An overall energy resolution between 10 and 15 keV was obtained. The target consisted of highly enriched (better than 99%) reactor-produced ^{59}Ni on a carbon backing. The thickness was about 45 $\mu\text{g}/\text{cm}^2$. Since the ^{59}Ni was deposited on the carbon foil with a mass separator, the target thickness was not very uniform.

A triton spectrum obtained at 6° is shown in Fig. 1. The spectra were analyzed by a peak-fitting program. In order to normalize the relative cross

sections at different angles, the beam on the target was monitored by recording, with a NaI scintillation counter, the protons elastically scattered at 90° from the target material. The absolute cross sections were obtained by normalizing to the elastic scattering of protons on ^{59}Ni obtained between 25° and 50° under the same experimental conditions as the (p, t) data. The measured elastic cross sections were assumed to have the values calculated with the optical model employing the parameters of Becchetti and Greenlees.¹⁰ The accuracy of the absolute cross sections thus determined is estimated to be $\pm 20\%$.

III. RESULTS

The excitation energies of the levels observed in the present experiment are given in Table I. They have been obtained by using a least squares fit to several calibration lines involving the impurities ^{13}C and ^{16}O and some low-lying levels of ^{57}Ni , the excitation energies of which are accurately known from γ -ray measurements. Included in Table I are data from the recent compilation of Auble.¹¹ Angular distributions were extracted for approximately 35 levels up to 9 MeV in excitation. They are displayed in Figs. 2-6 according to the exhibited L transfer. Our Q -value measurements for the $^{59}\text{Ni}(p, t)^{57}\text{Ni}$ and the $^{58}\text{Ni}(^3\text{He}, \alpha)^{57}\text{Ni}$ reactions leading to an improved value for the mass excess of ^{57}Ni were reported previously.¹²

A. Predominantly $L = 0$ transitions

The levels at 0.00, 3.01, 4.92 and 5.19 MeV are observed to be represented predominantly by $L = 0$ angular distributions. They are displayed in Fig. 2. For comparison, the $L = 0$ pattern of the $^{60}\text{Ni}(p, t)^{58}\text{Ni}$ ground state transition¹³ is superimposed as a dashed curve on the ground-state transition data. The observed $L = 0$ admixture determines a unique $J^\pi = 3/2^-$ assignment for these levels, since $J^\pi(^{59}\text{Ni} \text{ ground state}) = 3/2^-$.

B. Predominantly $L = 2$ transitions

Five levels with excitation energies up to 5.24 MeV are excited with predominantly $L = 2$ angular distributions. These transitions are shown in Fig. 3. The transition to the $1/2^-$ state at 1.11 MeV exhibits a pure $L = 2$ pattern consistent with the

$^{52}\text{Cr}(p,\alpha)^{49}\text{V}$ reaction

P. A. Smith,* J. A. Nolen, Jr., R. G. Markham, and M. A. M. Shahabuddin†

Cyclotron Laboratory and Physics Department, Michigan State University, East Lansing, Michigan 48824

(Received 18 November 1977; revised manuscript received 13 July 1978)

The $^{52}\text{Cr}(p,\alpha)^{49}\text{V}$ reaction has been studied at a bombarding energy of 35 MeV. The qualitative features of the spectra are discussed. These include the population of proton hole states, analog states, and high spin states. The spectra are compared with other pick-up reaction data and the comparison is shown to be a useful tool for identifying positive parity states in this region. Some states which are observed in $^{51}\text{V}(p,t)^{49}\text{V}$ data are not observed in the (p,α) spectra. Distorted-wave calculations using mass three cluster form factors are described and shown to reproduce the experimental angular distributions of the previously known levels. Similar calculations using microscopic form factors also reproduce the shapes of the angular distributions reasonably well. Relative spectroscopic factors for the proton hole states deduced from the microscopic calculations are shown to be in good agreement with zero order shell model predictions. The general trends of the experimental cross sections for the negative parity microscopic states are shown to be reproduced by microscopic calculations assuming $0f_{7/2}$ pick-up.

[NUCLEAR REACTIONS $^{52}\text{Cr}(p,\alpha)$, $E_p = 35$ MeV; measured $\sigma(E,\theta)$, deduced energy levels; studied reaction mechanism.]

I. INTRODUCTION

The (p,α) and (α,p) reactions may prove to be very useful spectroscopic tools. The qualitative features of these reactions are not well documented, with the exception of j -dependence for $\ell=1$ transfers.^{1,2,3,4} With the (p,α) reaction, for example, it is possible to study proton hole states in nuclei that are not accessible by other pick-up reactions, either because the targets for these reactions are unstable or difficult to make. Final nuclei in this class are ^{47}V , ^{51}Mn , ^{55}Co , ^{109}In , and ^{119}Sb . (Refs. 5-10) To understand the spectra of these nuclei, it is necessary to document the properties of the (p,α) reaction on nuclei that have been previously studied with simpler reactions. In this paper the qualitative features of the (p,α) reaction as seen in the $^{52}\text{Cr}(p,\alpha)^{49}\text{V}$ reaction are investigated. The $^{52}\text{Cr}(p,\alpha)^{49}\text{V}$ reaction is a good choice for such a study in the $0f_{7/2}$ shell because ^{49}V has been studied by a number of others.^{5,11-24}

Previous work in this mass region at beam energies above 17 MeV has shown that the simple proton hole states that are populated in single proton pick-up reactions dominate the (p,α) spectra (see references 2 and 25 for example). These states seem to be described reasonably well with seniority-one wave functions. Therefore, we should expect the ^{49}V spectrum to display strong peaks for the $7/2^-$ ground state and the $3/2^+$ and $1/2^+$ sd-shell proton hole states.

In addition to the $T=3/2$ proton hole states, the $T=5/2$ analogs of the hole states in ^{49}Ti should also be populated. These states are not isospin allowed in the $^{50}\text{Cr}(d,^3\text{He})^{49}\text{V}$ or the $^{50}\text{Cr}(t,\alpha)^{49}\text{V}$ reactions. Experimental observation of analog states with the (p,α) reaction has not been previously demonstrated except for some tentative assignments by Bardin and Rickey²⁶ with Ti targets, and the recent work of Smits and Siemssen.⁹

Multi-particle transfer direct reactions also have additional degrees of freedom which permit the population of high spin states.²⁷ For some time now the $(\alpha,xn\gamma)$ compound nuclear reactions have been used to populate such states, and recently heavy ion induced reactions such as $(^{19}\text{F},p2n\gamma)$ have been used to find high spin states such as the 12^+ in ^{44}Ti .²⁸ In the (p,α) reaction, if two $0f_{7/2}$

neutrons and a $0f_{7/2}$ proton are picked up, it is possible to reach final states via j^π transfers of up to $19/2^-$. The (p,α) reaction on ^{51}V could, in principle, directly populate a 12^+ state in ^{48}Ti . If the proton comes from the $0d_{3/2}$ orbit, $15/2^+$ is the maximum j^π transfer. A study of the $^{90,92,94,96}\text{Zr}(p,\alpha)^{87,89,91,93}\text{Y}$ reactions has concentrated on this aspect of the reaction.²⁹ Spins up to $15/2^-$ were observed in that work. The maximum coupling of $0d_{5/2}^+$, which is $13/2^+$, has been observed in $^{12}\text{C}(\alpha,p)^{15}\text{N}$, and $^{16}\text{O}(\alpha,p)^{15}\text{F}$ (see Refs. 30 and 31).

The best known feature of the (p,α) and (α,p) reactions is the strong j -dependence exhibited by $\ell=1$ transfers. The $1/2^-$ angular distribution is characterized by deep minima, while the $3/2^-$ angular distribution is featureless. This is an appealing feature for making j^π assignments for unknown states. Lee et al.¹ have shown that the j -dependence is a result of spin-orbit coupling in the proton optical potential. The j -dependence for the $j^\pi=1/2^-, 3/2^-$ spin-orbit pair is qualitatively reproduced by Distorted Wave Born approximation (DWBA) calculations independent of the details of the form factor used (see references 1, 3, 29 for examples). However, the reliability of j -dependence for high ℓ -values is not so clear. Studies of the $\ell=2$ and 3 transfers are confusing.^{4,32} Much of this confusion is apparently the result of important structure effects in the sd-shell. A study of the $^{24,26}\text{Mg}(p,\alpha)^{21,23}\text{Na}$ reactions shows that the angular distributions for states with the same j^π values sometimes have very different shapes.³³ It would seem that j -dependence will only be a useful tool in those mass regions where the shapes of the angular distributions are insensitive to the detailed structures of the states. This may be the case for targets that are heavier than those in the sd-shell.

The most common method of using the DWBA to predict the shapes of angular distributions of (p,α) and (α,p) studies has been with zero-range calculations employing mass three cluster form factors. For $A \geq 40$ these calculations fit the data reasonably well in most cases. In regions where nuclear structure does not affect the shapes of the angular distributions, it may be possible to use these calculations to make j^π assignments.^{29,34}

Microscopic reaction models for 3-nucleon transfer reactions have been developed, but they have not been

High-spin states in ^{146}Sm

C. H. King,* B. A. Brown, and T. L. Khoo†

Cyclotron Laboratory and Department of Physics, Michigan State University, East Lansing, Michigan 48824

(Received 18 November 1977)

Transitions between states up to spin $16\hbar$ populated in the $^{146}\text{Nd}(\alpha,4n)$ reaction were observed using γ - γ coincidence, γ -ray angular distribution and excitation function, and delayed γ -ray measurements. A level scheme was constructed up to 6.2 MeV with all levels above 3.8 MeV observed for the first time. Levels below 4.1 MeV were interpreted in terms of the coupling between two extra-core neutrons and excitations of the $N = 82$ core. Rotational structures and isomers were searched for above 4.1 MeV, but none were found.

NUCLEAR REACTIONS: $^{146}\text{Nd}(\alpha,4n\gamma)^{146}\text{Sm}$, $E=47.9$ MeV; measured E_γ , $I_\gamma(\theta)$, γ - γ coinc., α - γ delay, E_γ vs. E_α . ^{146}Sm deduced levels, J , π . Ge(Li) detectors. Enriched target.

I. INTRODUCTION

Efforts to achieve a consistent understanding of the properties of heavy nuclei a few nucleons removed from a closed shell have been largely unsuccessful. Various collective models have achieved some success in special cases, but no single model has yet been devised which can describe all such nuclei. It appears that the properties of these nuclei depend sensitively on the underlying single-particle structure, and it may be that an adequate description may require a more microscopic approach such as a large-basis shell model calculation. However, as yet calculations utilizing a sufficiently large basis have been largely confined to light nuclei.

The isotopes of samarium are among the most extensively investigated of these transitional nuclei, perhaps because the stable isotopes represent a wide range of nuclear properties from the spherical nuclide ^{144}Sm , which has a closed neutron shell, to ^{154}Sm , which appears to be a relatively conventional deformed nuclide. Of all the samarium isotopes, ^{146}Sm , ^{147}Sm , and ^{148}Sm ($N=84-86$) have been among the most resistant to understanding in any simple collective model. The known low-lying properties of these nuclides have revealed no rotational bands and for the most part vibrational band sequences appear to be absent as well. Nevertheless, calculations of Bengtsson et al.¹ have indicated that the yrast states of ^{146}Sm should become significantly deformed at relatively low spins, and moreover that the deformation should be oblate, thus favoring the existence of the oblate yrast traps which have been predicted by Bohr and Mottelson.² In addition, the existence of shape coexistence³ in the heavier samarium isotopes ^{150}Sm - ^{152}Sm ($N=88-90$) suggests the possibility of deformed structures appearing in the lighter isotopes at sufficiently high excitation energy.

We have therefore undertaken an investigation of high-spin states in the nuclides ^{146}Sm , ^{148}Sm using the $(\alpha,4n\gamma)$ reactions. The present paper reports the results of the ^{146}Sm investigation. Discussion of the ^{148}Sm results will appear in a subsequent report.⁴

II. EXPERIMENTAL PROCEDURE AND DATA ANALYSIS

The present study involved four separate measurements: 1) γ -ray angular distributions, 2) γ - γ coincidence, 3) γ -ray timing, and 4) γ -ray excitation functions. For all

measurements, the target was a foil of neodymium metal with approximately 6 mg/cm^2 areal density and enriched to 97.5% in ^{146}Nd . The angular-distribution, coincidence, and timing measurements were all performed using a 47.9-MeV alpha beam from the Michigan State University cyclotron.

The γ -ray angular distributions were measured using a coaxial Ge(Li) detector with approximately 40 cm^3 active volume, placed about 12 cm from target. Singles γ -ray spectra were obtained at seven angles between 90° and 157° with respect to the beam direction. A sample spectrum is shown in Fig. 1. Normalization was obtained by using another Ge(Li) detector fixed at -90° as a monitor, with deadtime corrections accomplished by feeding a beam-current digitizer output into the ADC's used for the pulse-height spectra of each detector. An effort was made to extract accurate γ -ray energies by performing separate runs with ^{75}Se , $^{166\text{m}}\text{Ho}$, ^{137}Cs , and ^{60}Co sources near the detector during the collection of a $^{146}\text{Nd} + \alpha$ spectrum and using the known⁵ energies of the lines in these sources to determine the energies of the $^{146}\text{Nd} + \alpha$ lines. The measured γ -ray energies listed in Table I are believed to be accurate to better than 0.1 keV for isolated peaks. The γ -ray excitation functions were obtained by taking singles spectra with the 40-cm^3 detector at a fixed angle of 125° for three other energies: 40, 45.8, and 49.8 MeV. For all spectra, photopeak areas were determined by using the peak-fitting program SAMPO.⁶

The angular distributions were fitted using the usual Legendre polynomial expansion:

$$W(\theta) = I_\gamma (1 + A_2 P_2(\cos\theta) + A_4 P_4(\cos\theta)).$$

The γ -ray intensities I_γ and the A_2 and A_4 coefficients are listed in Table I. It was found that for this, and a $^{148}\text{Nd}(\alpha,4n\gamma)^{148}\text{Sm}$ experiment performed at the same time, the extracted A_2 coefficients for known stretched-E1 and stretched-E2 transitions depopulating the same level were attenuated by significantly different amounts from the expected values for maximum alignment.⁷ However, a correction term of +0.05 added to the A_2 coefficients was found to yield consistent A_2 attenuation coefficients within uncertainties for all strong, well-resolved transitions. The A_2 coefficients listed in Table I have been corrected by this amount and an estimate of the uncertainty in this procedure is included in the quoted uncertainties. The attenuation factors for the extracted

Inner hole states in ^{207}Pb via the $^{208}\text{Pb}(^3\text{He},\alpha)^{207}\text{Pb}$ reaction at 70 MeV

S. Gales,* G. M. Crawley, D. Weber, and B. Zwieglinski†

Cyclotron Laboratory, Michigan State University, East Lansing, Michigan 48824

(Received 19 July 1978)

The $^{208}\text{Pb}(^3\text{He},\alpha)^{207}\text{Pb}$ reaction at 70 MeV incident energy was used to populate hole states up to 28 MeV excitation energy in ^{207}Pb . A split-pole spectrometer was used for particle analysis and detection. For the excitation energy range between 0 to 4.5 MeV, about eleven well resolved states are excited. These levels contain the main part of the spectroscopic strengths of the $3p_{1/2}$, $2f_{5/2}$, $3p_{3/2}$, $2f_{7/2}$, $1i_{13/2}$, and $1h_{9/2}$ neutron subshells. Three additional regions of enhanced cross sections, centered at 5.5, 8.5, and 14 MeV excitation energy in ^{207}Pb , are also observed. The 65 keV energy resolution of the present study revealed fine structure in the peak previously observed around 8.5 MeV in ^{207}Pb . About fifteen levels or groups of levels are populated between 4.5 and 10.5 MeV, and angular distributions have been extracted for each individual peak as well as for the gross structures. A distorted-wave Born-approximation analysis of the data was carried out and shows that the missing $l = 3$ and 5 strengths in ^{207}Pb are located in some strong peaks at 5.13, 5.62, and 6.37 MeV. Thus the full sum rule is obtained for the neutron subshells between $N = 126$ and $N = 82$. The highly fragmented peak located at 8.5 MeV excitation energy is shown to arise from $1h_{11/2}$ neutron pickup. Finally, the large structure, 5 MeV wide and centered around 14 MeV, observed for the first time in this work is tentatively interpreted as arising from neutron pickup from the $1g_{9/2}$ inner shell. The $T_>$ components of the deeply-bound state are also observed between 20 to 24 MeV in ^{207}Pb and therefore from the sum-rule analysis, centroid energies and total strengths for each inner subshell are deduced.

[NUCLEAR REACTION $^{208}\text{Pb}(^3\text{He}, \alpha)$, $E = 70$ MeV; measured $\sigma(E, \theta)$. ^{207}Pb deduced levels, E_x , l , (J) , π , C^2S ; inner shell spectroscopic factors; enriched target, magnetic spectrometer.]

I. INTRODUCTION

A number of experiments have been carried out in the past few years in order to populate inner hole states in heavy nuclei by means of neutron pickup reactions.¹⁻⁹ High energy light particle beams ($E \approx 40$ -200 MeV) have allowed the observation of a large range of excitation energy (up to 20-30 MeV) and have proved useful for the exploration of more deeply bound orbitals. Such experiments reveal that the particle group corresponding to the excitation of the inner shell is seen as a gross structure riding on a continuous background. A systematic study of this phenomena has been undertaken in the tin isotopes.^{1-3, 5-9} More recently the underlying fine structure of the $1g_{9/2}$ hole state was also observed using the (d,t) ⁵ and $(^3\text{He},\alpha)$ ⁹ reactions on $^{112,116,120}\text{Sn}$ with good energy resolution. Similar work has been carried out on ^{90}Zr and has allowed the observation of the inner $1f_{7/2}$ hole strength in ^{89}Zr .⁴ For heavier nuclei, most of the available data on the location and fragmentation of the neutron hole strength in the $N = 82$ (Nd and Sm isotopes for example) or $N = 126$ (Pb, Bi) mass regions involve a few well resolved states below 3.5 MeV excitation energy in the residual nuclei.¹⁰⁻¹² Only a few experiments have been performed in order to investigate neutron pickup from the inner shells in these nuclei. In particular, a systematic study of the fragmentation of the $h_{11/2}$ neutron orbital in Nd and Sm isotopes has been published recently.¹³ For the lead region, Lewis¹⁴ has observed a broad structure around 8 MeV in ^{207}Pb in the study of the $^{208}\text{Pb}(^3\text{He},\alpha)$ reaction at 75 MeV and interpreted this enhancement of the cross-section as arising from the $h_{11/2}$ neutron hole strength in this nucleus. In addition, the calculated shape of the excitation energy spectrum in ^{207}Pb shows that the tail of this bump could also arise from neutron pickup from much

deeper orbitals ($1g_{9/2}$, for example). The systematic study of the $(^3\text{He},\alpha)$ reaction at 205 MeV incident energy on nuclei ranging from ^{12}C to ^{208}Pb has confirmed the existence of this broad bump at 8.3 MeV excitation energy in ^{207}Pb , together with the population of much narrower unknown states at 4.2, 5.1, and 6.1 MeV.⁶ However, in both cases these studies suffer from a lack of good energy resolution ($\Delta E \approx 400$ keV FWHM). The precise determination of l values for the narrow states located between 4.5 and 6.5 excitation energy together with the possible existence of underlying fine structure in the broad bump near 8 MeV could not be investigated under these conditions.

Finally, at much higher excitation energy ($E_x \approx 20$ MeV) one expects to populate the $T_>$ components of such deeply bound states, although the large isospin quantum number of these levels, $T_> = 45/2$, leads to a strong reduction of the single hole cross-section ($d\sigma/d\Omega \propto 1/2T_>$). The observation of both components ($T_<$ and $T_>$) of the deeply bound states in the lead region is of importance due to the simple nature of these states and provides unique information on both the nuclear structure and the reaction mechanism.

In the present high resolution (65 keV full width at half maximum (FWHM) for 83 MeV α -particles) study of the $^{208}\text{Pb}(^3\text{He},\alpha)$ reaction investigated at 70 MeV incident energy, hole states with high l values over a wide range of excitation energy (≈ 28 MeV) were investigated in the ^{207}Pb residual nucleus. Both the low-lying states and the levels, located at higher excitation energy, which carry the strength of the $1h_{9/2}$, $1h_{11/2}$, and possibly $1g_{7/2}$ and $1g_{9/2}$ inner neutron orbitals were observed. A short report on the observation of the hole-analog states in ^{207}Pb has been recently published elsewhere.¹⁵ Therefore only the results obtained from that previous analysis will be used here to deduce the centroid energies

$^{208}\text{Pb}(p, \alpha)^{205}\text{Tl}$ reaction

P. A. Smith

Nuclear Physics Laboratory Department of Physics and Astrophysics, University of Colorado, Boulder, Colorado 80309

G. M. Crawley, R. G. Markham, and D. Weber

Cyclotron Laboratory, Michigan State University, East Lansing, Michigan 48824

(Received 12 June 1978)

The $^{208}\text{Pb}(p, \alpha)^{205}\text{Tl}$ reaction has been studied at $E_p = 35$ MeV. Excitation energies and angular distributions have been obtained for many new states in ^{205}Tl . Cluster model distorted-wave Born approximation calculations are shown to produce excellent fits to the angular distributions. Among the new states, four are given $(15/2, 17/2)^+$ assignments and one is assigned as $(19/2, 21/2)^+$ on the basis of the distorted-wave Born approximation fits.

NUCLEAR REACTIONS $^{208}\text{Pb}(p, \alpha)$, $E_p = 35$ MeV; measured $\sigma(\theta)$; ^{205}Tl deduced levels; enriched target, DWBA analysis; compared with weak coupling model.

I. INTRODUCTION

The spectra of nuclei near the ^{208}Pb double shell closure provide an unusually attractive testing ground for nuclear structure models. In particular, those nuclei which are three particles (a combination of nucleons and nucleon holes) away from the $Z = 82$, $N = 126$ boundary provide a sensitive test for empirical shell model calculations, where the two-body matrix elements are taken from the two particle spectra and the single particle energies are deduced from the levels of ^{207}Tl , ^{207}Pb , ^{209}Bi , and ^{209}Pb . Such a calculation for ^{205}Tl would proceed by taking the n - n interactions from the ^{206}Pb spectrum and the p - n interactions from the ^{206}Tl spectrum, while the proton and neutron hole energies would come from ^{207}Tl and ^{207}Pb . Extensive shell model calculations for three particle nuclei near ^{208}Pb have been presented by a Stockholm group, along with a wealth of data obtained from γ -ray decay experiments.¹⁻⁵ They find outstanding agreement especially for the high spin states. Their study has not included ^{205}Tl , which should be one of the simplest shell model calculations, presumably because the large neutron excess makes it a difficult nucleus to reach with fusion-evaporation reactions.

The $^{208}\text{Pb}(p, \alpha)^{205}\text{Tl}$ reaction is ideal for locating high spin states in ^{205}Tl . Direct three nucleon transfer reactions on targets near ^{40}Ca have been found to populate high spin states that have simple shell model wave functions.⁶ Total angular momentum transfers as large as $19/2$ have been reported with good agreement between the experimental angular distributions and the shapes predicted by distorted wave Born approximation (DWBA) calculations. We can therefore expect to locate some of the high spin states in ^{205}Tl by comparing the experimental (p, α) angular distributions with DWBA calculations.

The low-lying states in ^{205}Tl may also be described with a weak, or intermediate, coupling model where an $s_{1/2}$ or $d_{3/2}$ proton hole is coupled to the 0^+ , 2^+ , and 4^+ states of ^{206}Pb . Once again the (p, α) reaction is an ideal way to locate the members of this coupling scheme because the "triton" pickup excites both the neutrons and protons. By comparison, proton pickup is a poor way to locate all the members of the scheme since nearly all the proton-hole spectroscopic factors will lie in one state, if the coupling is weak. By comparing the (p, α) results presented here to the (t, α) results of Flynn *et al.*,⁷ we

should be able to test the weak coupling scheme for the low-lying ^{205}Tl spectrum.

In the sections that follow, we will present the data obtained for the $^{208}\text{Pb}(p, \alpha)^{205}\text{Tl}$ reaction at $E_p = 35$ MeV. The angular distributions will be compared with DWBA calculations to place limits on J^π values and to assign high spin state l values. The resulting picture of ^{205}Tl will be discussed, in terms of simple empirical shell model calculations and weak coupling considerations.

II. EXPERIMENT AND DATA

A beam of 35 MeV protons from the Michigan State University cyclotron was used to bombard a $40 \mu\text{g}/\text{cm}^2$ target of isotopically enriched ^{208}Pb which was deposited by evaporation onto a $20 \mu\text{g}/\text{cm}^2$ carbon foil. The lead thickness was determined by comparing the elastic scattering angular distribution to an optical model calculation. The reaction products were analyzed with an Enge split-pole spectrograph and the Markham-Robertson focal plane detector⁸ backed by a plastic scintillator. The α particles were uniquely identified by their energy loss in the counter gas and by their time-of-flight relative to the cyclotron radio frequency. In addition to the counter spectra, one run was recorded on a photographic emulsion for the purpose of obtaining more precise excitation energies than could be derived from the counter data. The energy resolution for the plate run was about 15 keV full width at half maximum (FWHM).

Two typical counter spectra with an energy resolution of about 25 keV FWHM and collected for about the same charge are shown in Fig. 1. Two features of the data are evident. The first is the extreme forward peaking of the angular distributions for the low-lying states, as can be seen by comparing the size of the ground state peak in the upper and lower portions of the figure. The second is the emergence of the large peak in the back angle spectra.

III. RESULTS

A. Levels Observed

The excitation energies deduced from the current (p, α) data are given in Table I along with those found in the literature. For the most part, the (p, α) energies were determined from the plate data. The calibration lines were taken from the low-lying states that have been

Interpretation of the anomalous electron-capture to positron decay ratio in $^{22}\text{Na}^\dagger$

R. B. Firestone and Wm. C. McHarris

Department of Chemistry, Cyclotron Laboratory and Department of Physics, Michigan State University, East Lansing, Michigan 48824

Barry R. Holstein

Physics Division, National Science Foundation, Washington, D. C. 20550

(Received 17 January 1978; revised manuscript received 13 October 1978)

The impact of second-forbidden corrections is studied in order to relate the ϵ/β^+ ratio, the spectral shape factor, and the β - γ directional correlation measurements in ^{22}Na decay.

[RADIOACTIVITY ^{22}Na ; second-forbidden corrections to β -decay calculations.]

I. INTRODUCTION

The electron-capture to positron decay branching ratio (hereafter ϵ/β^+) for ^{22}Na was measured originally in order to test for Fierz interference.¹ The allowed theory of β decay had been well established, and theoretical ϵ/β^+ ratios could be readily calculated. Early experiments indicated that experiment and theory agreed to within several percent,² and this was used as evidence against the existence of Fierz terms.

The ^{22}Na ϵ/β^+ ratio has since been remeasured by several groups, leading to five especially precise results,³⁻⁷ which are shown in Table I. The first three results agree quite closely, and, although the fourth result differs from the others, it too is in significant disagreement with theory. The fifth result, although in agreement with theory, is a less direct measurement because it relies on tabulated detector efficiencies. In addition, this result is quite sensitive to small amounts of γ -ray attenuation in the absorbers near the source. Until it is understood why this result differs so drastically, we shall take the point of view that a possible substantial deviation exists, and we

shall in the calculations discussed below (which stand apart from the experimental uncertainties) consider the theoretical conclusions implied by such large deviations from allowed theory.

Experimental data also exist on the ^{22}Na β spectral shape and β - γ directional correlation, both of which are sensitive to Fierz interference and/or second-forbidden effects. Several authors have precisely measured the ^{22}Na spectral shape.⁸⁻¹¹ Wenninger, Stiewe, and Leutz⁸ published their raw data which we have examined below, while the other authors generally reported a $1/E$ dependence. The resulting linear slopes between $100 \text{ keV} \leq E_\beta \leq 400 \text{ keV}$ are presented in Table II. These values are consistent with the slope being near zero. The results were originally analyzed to show the absence of a Fierz term; however, the analysis did not contain second-forbidden form factors, which, in view of the very hindered nature of this decay, could be rather significant.¹² Finally, two precise values of the ^{22}Na β - γ directional correlation coefficient A_{22} have been measured^{13,14} and are given in Table III. Although these values are not entirely consistent with each other, they both seem consistent with $A_{22} \leq 0$.

TABLE I. ^{22}Na experimental ϵ/β^+ decay branching ratios.

ϵ/β^+	ν , skew ratio	Ref.
0.1048 ± 0.0007	0.910 ± 0.008	Leutz and Wenninger (1967), Ref. 4
0.1042 ± 0.0010	0.905 ± 0.011	Vatai, Varga, and Uchirin (1968), Ref. 5
0.1041 ± 0.0010	0.904 ± 0.011	Williams (1964), Ref. 3
0.1077 ± 0.0006	0.935 ± 0.008	MacMahon and Baerg (1976), Ref. 6
0.1128 ± 0.0018	0.979 ± 0.018	Bosch <i>et al.</i> , Ref. 7.
0.1152 ± 0.0003	...	Theory—this paper

Communications

The Communications section is for brief reports on completed research. A Communication may be no longer than the equivalent of 2800 words, i.e., the length to which a Physical Review Letter is limited. (See the editorial in the 21 December 1970 issue of Physical Review Letters.) Manuscripts intended for this section must be accompanied by a brief abstract for information retrieval purposes and a keyword abstract.

α -transfer spectroscopic factors in ^{23}Na

W. Chung

IKP, KFA Julich GmbH, Postfach 1913, D-5170, Julich, West Germany

H. T. Fortune

Physics Department, University of Pennsylvania, Philadelphia, Pennsylvania 19104

B. H. Wildenthal

Cyclotron Laboratory, Michigan State University, East Lansing, Michigan 48824

(Received 10 October 1978)

α -transfer spectroscopic factors computed from shell-model wave functions for ^{19}F and ^{23}Na generated in the full sd -shell model space with the Chung-Wildenthal interaction are in good agreement with experimental $^{19}\text{F}(^6\text{Li}, d)^{23}\text{Na}$ results, contrary to previous SU(3)-type calculations.

[NUCLEAR STRUCTURE ^{23}Na ; Calculation of α spectroscopic factors in full sd basis; comparison with experiment and SU(3).]

In a recent study¹ of the reaction $^{19}\text{F}(^6\text{Li}, d)^{23}\text{Na}$, relative α -transfer spectroscopic factors S_α were found to be in serious disagreement with both pure SU(3) predictions² and with results of a shell-model calculation¹ that included only leading SU(3) representations in the model space. Among the major difficulties were the following:

(1) For the ground-state $K = \frac{3}{2}$ band, the predicted relative α -transfer spectroscopic strengths for the two J values of each L transfer disagreed with the experimental results, i.e., the predictions as to which member of each pair was more strongly populated disagreed in each case with experiment.

(2) The first $\frac{1}{2}^+$ state, at 2.39 MeV, observed experimentally to be strong, was predicted to have zero strength, whereas the second $\frac{1}{2}^+$ state, at 4.43 MeV, was observed to be weak but predicted to be strong.

(3) Relative to the average of all the other states, the observed ground state α -transfer spectroscopic strength was much stronger than predicted.

Recently, theoretical α -transfer spectroscopic factors for sd -shell nuclei calculated from wave functions generated in the full sd -shell model space have been reported³ for transitions between all pairs of experimentally accessible ground

states. Using the same method and set of consistent wave functions⁴ as in Ref. 3, we have calculated α -transfer spectroscopic factors for the reaction $^{19}\text{F}(^6\text{Li}, d)^{23}\text{Na}$. The results are found to be

TABLE I. Excitation energies and S_α 's for ^{23}Na .

E_x (MeV)		J^π	$(^6\text{Li}, d)$	S_α	
Exp.	Calc.			Full- sd	SU(3) ^a
0.0	0.0	$\frac{3}{2}^+$	1.0	1.0	1.0
0.44	0.39	$\frac{5}{2}^+$	0.40	0.78	3.38
2.08	2.15	$\frac{1}{2}^+$	1.98	2.81	2.29
2.39	2.14	$\frac{1}{2}^+$	4.0	5.02	0.0
2.70	2.76	$\frac{3}{2}^+$	0.66	1.39	5.83
2.98	2.83	$\frac{3}{2}^+$	0.85	0.64	3.75
3.92	3.70	$\frac{5}{2}^+$	(1.12)	6.68	1.37
4.43	4.37	$\frac{1}{2}^+$	0.54	2.05	6.67
4.78	4.69	$\frac{1}{2}^+$	1.44	3.17	6.53
5.38	5.41	$(\frac{5}{2}^+)$	0.34	0.01	3.52
5.54	5.64	$\frac{11}{2}^+$	(1.84)	0.75	0.89
6.23	6.21	$\frac{13}{2}^+$...	0.49	2.67

^a Reference 2.

Distribution of particles in Fermi systems

G. Bertsch and J. Borysowicz

Physics Department and Heavy Ion Laboratory, Michigan State University, East Lansing, Michigan 48824

(Received 4 October 1978)

We show that the number of particles within a subvolume of a finite Fermi system has a variance that scales with the number of particles as $N^{2/3} \log N$. This contrasts with the naive classical model, which gives a scaling proportional to N . It also contrasts with a certain collective model that produces a variance that scales as $N^{2/3}$.

NUCLEAR STRUCTURE, NUCLEAR REACTIONS nuclear matter, bulk matter and collective aspects of heavy-ion reactions, general properties of fission.

It is possible to imagine experiments in which the number of particles in a certain subvolume of an extended Fermi system are measured. For example, in high energy heavy ion collisions, the projectile would shear off a large chunk of the target, and the number of nucleons in the remaining piece could, in principle, be measured. The question arises as to the distribution of nucleon number to be expected. Bondorf *et al.*¹ have considered this question and calculated a theoretical variance within a simple collective model.

A first guess for the variance might be the independent particle classical limit. Here the variance σ^2 for a measurement of the number of particles within a certain subvolume would satisfy

$$\sigma^2 \equiv \langle n^2 \rangle - \langle n \rangle^2 = Np(1 - p), \tag{1}$$

where N is the total number of particles being considered, and $p = \langle n \rangle / N$ is the probability that a particle is in the volume. In Ref. 1 the variance found is considerably smaller.

The variance can be computed quantum mechanically in terms of the two-body density. It appears to be a remarkable feature of Fermi systems that the Pauli principle reduces the fluctuations drastically, changing the dependence on $\langle n \rangle$ to

$$\sigma^2 \sim \langle n \rangle^{2/3} \log \langle n \rangle. \tag{2}$$

We shall derive this result for a Fermi gas wave function. In Ref. 1 an approximation is made which results in a dependence of the variance as $\langle n \rangle^{2/3}$. These authors also suggest that a more rapid dependence than $\langle n \rangle^{2/3}$ might be closer to reality.²

It is first necessary to write down the expression for the variance in a measurement of single-particle projection operator, Θ . For a determinantal wave function built up out of single-particle orbits j, k the variance is given by

$$\sigma^2 \equiv \langle \Theta^2 \rangle - \langle \Theta \rangle^2 = \sum_{jk} \langle j | \Theta | k \rangle \langle k | (1 - \Theta) | j \rangle. \tag{3}$$

We apply this to a Fermi gas in a box of side L , using plane waves and periodic boundary conditions. The single-particle wave functions have the form

$$\phi_j(\vec{r}) = \frac{1}{L^{3/2}} e^{i\vec{k}_j \cdot \vec{r}}, \quad -L/2 \leq r_{x,y,z} \leq L/2. \tag{4}$$

The momentum vector k_j is given in terms of Cartesian quantum numbers n^j by

$$\vec{k}_j = \frac{2\pi}{L} (n_x^j, n_y^j, n_z^j). \tag{5}$$

For the ground state of the Fermi gas, these quantum numbers satisfy

$$n_x^2 + n_y^2 + n_z^2 \leq n_F^2. \tag{6}$$

The number of particles of a given kind N is approximately

$$N = \frac{4\pi}{3} n_F^3. \tag{7}$$

For our projection operator, we consider the number of nucleons on one side of the xy plane. The single-particle matrix elements are given by

$$\langle j | n(z > 0) | k \rangle = P_{jk} \delta_{n_x^j, n_x^k} \delta_{n_y^j, n_y^k}$$

with

$$P_{jk} = \frac{1}{L} \int_0^{L/2} dz \exp[-(2\pi i/L)(n_x^j - n_x^k)z] = \begin{cases} \frac{1}{2} & n_x^j = n_x^k \\ \frac{1}{(n_x^j - n_x^k)\pi i} & n_x^j - n_x^k \text{ odd} \\ 0 & n_x^j - n_x^k \text{ even, } \neq 0. \end{cases} \tag{8}$$

Inserting the explicit value of the diagonal matrix elements into Eq. (3), the variance becomes

g-factor of the $19/2^-$ isomer in ^{115}Sb

S. R. Faber, L. E. Young,* and F. M. Bernthal

Departments of Chemistry and Physics, and Cyclotron Laboratory, Michigan State University, East Lansing, Michigan 48824
(Received 6 October 1978)

The g factor of the $t_{1/2} = 156$ nsec $19/2^-$ isomer in ^{115}Sb was measured by the time differential perturbed angular distribution technique using the reaction $^{115}\text{In}(\alpha, 4n)^{115}\text{Sb}$. The measured value $g = +0.287(4)$ agrees with the structure $[\nu h_{11/2} \otimes \nu d_{3/2} \otimes \pi d_{5/2}]_{9/2^-}$ assuming additivity. The g factor of the $11/2^-$ $t_{1/2} = 6.2$ ns state fed by the $19/2^-$ isomer decay was found to be $+1.06(10)$.

[NUCLEAR REACTIONS $^{115}\text{In}(\alpha, 4n)$, $E_\alpha = 48$ MeV, pulsed beam, measured $I_\gamma(\theta, B, t)$ for $E_\gamma = 1217, 1300$ keV, spin rotation; deduced $g_{19/2^-}$, $g_{11/2^-}$]

I. INTRODUCTION

The nucleus ^{115}Sb lies in a shape transitional region. It is one proton outside the $Z = 50$ closed shell and exhibits some vibrational states similar to the neighboring Sn nuclei, but it also has a rotational band built on the $9/2^+[404]$ Nilsson state.¹ The nonrotational part of the spectrum has been explained by coupling a $d_{5/2}$ proton to excited states of the ^{114}Sn core.² Recently an in-beam γ -ray study of ^{115}Sb yielded data on high spin states in that nucleus.³ Three isomers were seen: a $t_{1/2} = 6.7$ ns $11/2^-$ isomer at 1300.2 keV, a 156 ns $19/2^-$ isomer at 2796.3, and a 4.0 ns $25/2^-$ isomer at 3059.7 keV corresponding to a $d_{5/2}$ proton coupled to the ^{114}Sn $3^-, 7^-$, and 10^+ states, respectively. Figure 1 shows a partial decay scheme involving those isomers. The $19/2^-$ isomer is thought to be a three particle state $[\pi d_{5/2} \otimes \nu h_{11/2} \otimes \nu d_{3/2}]$, where $[\nu h_{11/2} \otimes \nu d_{3/2}]$ is the 7^- state in the ^{114}Sn core. According to Bron³ the wave function probably contains some admixture of $(\pi h_{11/2} \otimes 4^+)$ since the transition $19/2^-$ to $11/2^-$ in ^{115}Sb is enhanced about a factor of three over the corresponding 7^- to 5^- transition in ^{114}Sn . The measurement of the g -factor could give an indication of the extent of the admixture.

Recently the g -factor of the $11/2^-$ isomer in ^{115}Sb has been measured by Ketel *et al.*⁴ They obtained a value of 0.97 (10) using a $^{116}\text{Sn}(p, 2n)^{115}\text{Sb}$ reaction and suggested the state was a mixture of $\pi h_{11/2}$ and $\pi d_{5/2} \otimes 3^-$ (octupole vibration). In that reaction little or no population of the higher lying $19/2^-$ isomer occurs, and thus a direct time differential perturbed angular distribution measurement can be made of the $11/2^-$ state. In this experiment the 1300 keV transition is complicated by the higher lying isomer requiring careful analysis to extract an accurate g -factor for the $11/2^-$ state.

II. EXPERIMENT

The g -factors were measured using the time differential perturbed angular distribution technique (TDPAD). The reaction was $^{115}\text{In}(\alpha, 4n\gamma)^{115}\text{Sb}$, induced by a 48 MeV α particle beam from the MSU cyclotron. The target was a thick (110 mg/cm²) natural metallic In foil (95.7% ^{115}In). Indium is a good host lattice for the ^{115}Sb recoils due in part to its tetragonal lattice structure which maintains the alignment over several precession cycles. The low melting point of In (156°C) insures a high mobility of lattice defects induced by the beam even at room temperature and thus reduces the main cause of loss of alignment generally experienced with this technique.

The magnet used produced a 22.7 kG magnetic flux density with less than 0.5% deviation over the target area. The field was calibrated to less than 1% error using a flip coil that had been calibrated with nuclear magnetic resonance. Two 10% efficient Ge(Li) detectors were placed at $\pm 135^\circ$ to the beam. The beam was chopped with an electrostatic deflector so there were 526 ns between bursts. Six energy gates were set per detector, one on the 1217 keV line, one on the 1300 keV line, and two background gates, one on either side of each peak.

Figure 2 shows the background subtracted time to amplitude converter (TAC) spectra and the normalized sum spectra formed by adding the spectra from the two detectors. The 1300 keV transition is a doublet containing some of the 1294 keV line from ^{116}Sb decay. The amount of this background in each 1300 keV spectrum was determined by fitting each TAC spectrum to the equation for a time spectrum incorporating the 156 ns half-life as determined from the 1217 keV sum TAC, plus a background due to the 15 min

α -particle spectroscopy in Ni and Zn

C. L. Bennett* and H. W. Fulbright

Nuclear Structure Research Laboratory, University of Rochester, Rochester, New York 14627

J. F. A. van Hienen†, W. Chung‡, and B. H. Wildenthal

Cyclotron Laboratory, Michigan State University, East Lansing, Michigan 48824

(Received 10 August 1978)

α particle spectroscopic factors have been calculated in the $f_{5/2}p_{3/2}p_{1/2}$ shell model space for transitions from the Ni isotopes to states in $^{62,64,66,68}\text{Zn}$. The Zn ground states are found to be described well by weak-coupling $^{60}\text{Zn}_{g.s.}$ to the corresponding Ni ground state.

[NUCLEAR STRUCTURE Calculated α spectroscopic factors in shell model for even Ni + $\alpha \rightarrow$ Zn, compared with Ni($^6\text{Li}, d$)Zn S values.]

Until recently it has been impractical to attempt detailed jj coupled shell model calculations involving many-body correlations, e.g., calculations of multinucleon transfer spectroscopic factors. Computers and codes now exist for doing large scale shell model calculations,¹ as do computer-accessible multiparticle coefficients of fractional parentage² (CFP's), so detailed shell model calculations of such complex quantities have become feasible. We consider here the calculation of α -particle transfer spectroscopic factors and evaluate measures of the goodness of weak-coupling descriptions of some of the Ni and Zn isotopes. Calculated values of α -particle spectroscopic factors will be compared with experimental values of reduced α transfer cross sections from ($^6\text{Li}, d$) work (Ref. 3).

The basis used for all of the present calculations is the full $(f_{5/2}p_{3/2}p_{1/2})^n$ shell model space. The wave functions for the Ni and Zn nuclei are those of Ref. 4, obtained by diagonalizing the adjusted surface delta interaction (ASDI). The ASDI was derived by Koops and Glaudemans⁵ from the modified surface delta interaction (MSDI)⁶ by varying the two-body matrix elements to fit selected energy levels in the Cu and Ni isotopes. In the calculation of α -particle spectroscopic factors, three different sorts of wave functions to be described later were used to represent the α transfer operator.

In simplified notation, with angular momentum labels etc. suppressed, the amplitude for adding an α -particle to state A and reaching state B is proportional to the reduced matrix element $\langle B||\alpha||A \rangle$. With wave functions for A, α , and B given by

$$|B\rangle = \sum_i c_i |i\rangle,$$

$$|\alpha\rangle = \sum_j c_j |j\rangle,$$

$$|A\rangle = \sum_k c_k |k\rangle,$$

then

$$\langle B||\alpha||A \rangle = \sum_i \sum_j \sum_k c_i c_j c_k \langle i||j||k \rangle.$$

In the above $|i\rangle$, $|j\rangle$, $|k\rangle$ are multishell basis states in the space of B, α , and A, respectively, and $\langle i||j||k \rangle$ is the multishell reduced matrix element connecting the indicated basis states. A more detailed description of this formalism is contained in Ref. 2. The wave function $|\alpha\rangle$ of the transferred nucleon group will generally have center of mass motion described by a form factor $\phi_L(r_{\alpha A})$ which may be a superposition of form factors having different numbers of radial nodes.

More generally, the correlation between a state B and a coupled product of the arbitrary states α and A may be described in terms of the scalar product

$$\hat{B} \cdot (\alpha \hat{\otimes} A),$$

where $(\alpha \hat{\otimes} A)$ represents the unit vector formed by coupling the state α to the state A, i.e., the i th component of the unnormalized coupled product is

$$(\alpha \hat{\otimes} A)_i = \sum_j \sum_k c_j c_k \langle i||j||k \rangle = \langle i||\alpha||A \rangle$$

Parity of $^{19}\text{F}(5.10)$ and $^{19}\text{Ne}(5.09)$

H. T. Fortune and J. N. Bishop*

Physics Department, University of Pennsylvania, Philadelphia, Pennsylvania 19104

H. Nann† and B. H. Wildenthal

Cyclotron Laboratory, Michigan State University, East Lansing, Michigan 48824

(Received 28 August 1978)

Data for $^{17}\text{O}(^3\text{He},p)^{19}\text{F}$ and $^{21}\text{Ne}(p,t)^{19}\text{Ne}$ establish the parity of the 5.10 and 5.09 MeV levels in ^{19}F and ^{19}Ne , respectively, as positive, and are consistent with the earlier assignments of $J = 5/2$.

[NUCLEAR REACTIONS $^{17}\text{O}(^3\text{He},p)$, $E = 18.0$ MeV; $^{21}\text{Ne}(p,t)$, $E = 40$ MeV; ^{19}F , ^{19}Ne levels deduced L, π . DWBA analysis. Enriched targets.]

The state at 5.10 MeV in ^{19}F has a $J^\pi = \frac{5}{2}^-$ assignment in the latest compilation.¹ The $\frac{5}{2}$ assignment^{2,3} appears firm, but a variety of reactions give ambiguous results on the parity. It is seen^{4,5} with $l = 2$ or 3 in $^{18}\text{O}(^3\text{He},d)$. Inelastic scattering gives conflicting results: $L = 3$ in (α, α') ⁶ and a preference for $L = 2$ in (p, p') .⁷ Gamma decays³ prefer positive parity.⁸ We report here on data that appear to establish positive parity for it and its mirror at 5.09 MeV in ^{19}Ne .

Figure 1 displays an angular distribution for the reaction $^{17}\text{O}(^3\text{He},p)^{19}\text{F}$ together with a comparison with a variety of distorted-wave Born-approxima-

tion (DWBA) curves. If the state has $J^\pi = \frac{5}{2}^-$, it should be reached in $(^3\text{He}, p)$ via odd L values. Yet no combination of curves for odd L can give an adequate account of the data. The forward rise in the angular distribution is too steep to be fitted with odd L . However, an admixture of $L = 0$ and 2 provides an excellent fit. The results are the same if empirical shapes, rather than DWBA curves, are used to fit the data. The mixture of $L = 0$ and 2 is consistent with $J = \frac{5}{2}$ and requires positive parity.

Figure 2 displays an angular distribution for the reaction $^{21}\text{Ne}(p,t)$ leading to the mirror state in ^{19}Ne . Again, curves for odd L give a very poor account of the data, whereas an $L = 4$ curve provides an excellent fit. These data then strongly suggest that the ^{19}Ne level also has positive parity.

We thus conclude that the parity of $^{19}\text{F}(5.10)$ and

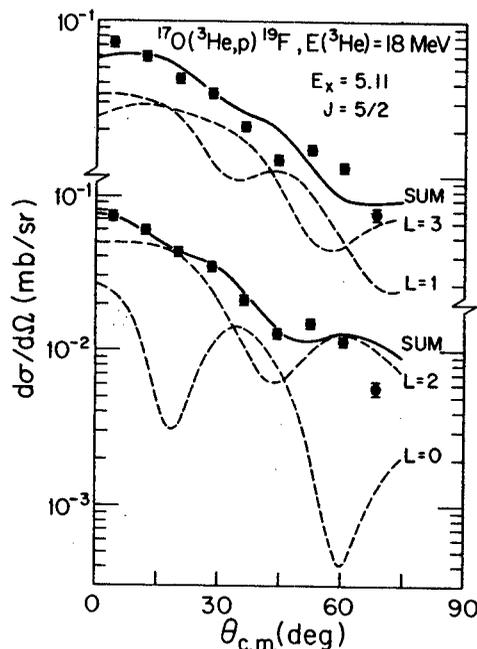


FIG. 1. Angular distribution of the $^{17}\text{O}(^3\text{He},p)$ reaction leading to the $J = \frac{5}{2}$ level at 5.10 MeV excitation in ^{19}F . Data are fitted with DWBA curves for odd L (top) and even L (bottom).

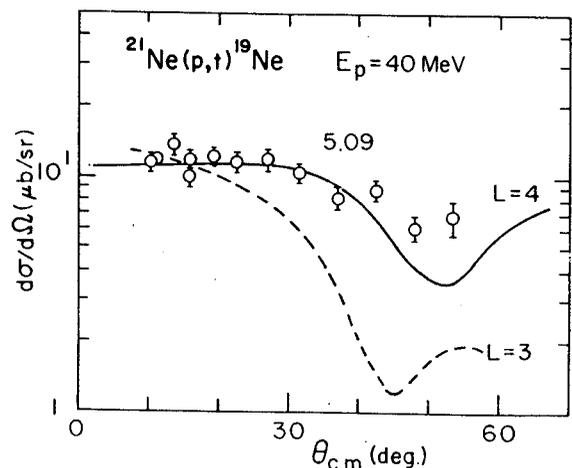


FIG. 2. Angular distribution of the $^{21}\text{Ne}(p,t)$ reaction populating the $J = \frac{5}{2}$ level at 5.09 MeV in ^{19}Ne , compared with DWBA curves for $L = 4$ (solid) and $L = 3$ (dashed).

(p, t) and $(p, {}^3\text{He})$ reactions on ${}^{33}\text{S}$

H. Nann*

Cyclotron Laboratory, Michigan State University, East Lansing, Michigan 48824
and Northwestern University, Evanston, Illinois 60201

B. H. Wildenthal

Cyclotron Laboratory and Department of Physics, Michigan State University, East Lansing, Michigan 48824
(Received 27 November 1978)

Angular distributions of the ${}^{33}\text{S}(p, t){}^{31}\text{S}$ and ${}^{33}\text{S}(p, {}^3\text{He}){}^{31}\text{P}$ reactions have been measured at 40 MeV bombarding energy. Unambiguous spin parity assignments of $3/2^+$ are made to levels in ${}^{31}\text{S}$ at 3.44, 4.53, and 6.27 MeV excitation energy on the basis of the observed $L = 0$ admixtures in their angular distributions. The lowest $T = 3/2$ state in ${}^{31}\text{S}$ was observed and its excitation energy determined to 6.268 ± 0.010 MeV. The experimental differential cross sections of transitions to low-lying mirror pairs of even parity final states in ${}^{31}\text{S}$ and ${}^{31}\text{P}$ are compared to the results of microscopic distorted-wave Born-approximation calculations based on shell-model calculations.

NUCLEAR REACTIONS ${}^{33}\text{S}(p, t)$, ${}^{33}\text{S}(p, {}^3\text{He})$, $E_p = 40$ MeV; measured $\sigma(E_t, E_{{}^3\text{He}}, \theta)$; enriched target, deduced L, J, π values, measured Q of lowest $T = \frac{3}{2}$ level in ${}^{31}\text{S}$; DWBA analysis.

I. INTRODUCTION

The present study of the ${}^{33}\text{S}(p, t)$ and ${}^{33}\text{S}(p, {}^3\text{He})$ reactions is a part of a systematic investigation of the (p, t) and $(p, {}^3\text{He})$ reactions on $T_z = \frac{1}{2}$ nuclei in the $2s-1d$ shell¹⁻³ with the aim of testing two-particle correlations in shell-model wave functions. Owing to the different selectivity of the two reactions, different parts of the initial and final state wave functions can be sampled in the mirror transitions. Shell-model wave functions for the nuclei studied here have been recently calculated by Chung and Wildenthal⁴ in the full $2s-1d$ shell basis space. The two-body matrix elements were treated as independent free parameters adjusted to fit experimental ground state binding energies and level spacings. Microscopic distorted-wave Born approximation (DWBA) calculations based on spectroscopic amplitudes calculated from these wave functions were used to predict relative (p, t) and $(p, {}^3\text{He})$ cross sections of mirror transitions. The consistency of the ratio of the measured to calculated cross sections as well as the agreement in shape then gives a measure of the extent to which the theoretical wave functions are a correct formulation of the actual nuclear structure.

II. EXPERIMENTAL PROCEDURE AND RESULTS

The present experiments were performed with a 40 MeV proton beam from the Michigan State University cyclotron. The reaction products were detected in a position-sensitive wire counter plas-

tic-scintillator combination in the focal plane of an Enge split-pole spectrograph. This equipment provided excellent particle identification and an energy resolution of about 30 keV. The target consisted of one layer of enriched ${}^{33}\text{S}$ (22.3% ${}^{33}\text{S}$, 76.8% ${}^{32}\text{S}$, and 0.9% ${}^{34}\text{S}$), sandwiched between layers of Formvar and carbon foils in order to inhibit evaporation during the bombardment. The target thickness was about $15 \mu\text{g}/\text{cm}^2$. Throughout the experiment the target thickness was monitored by the continuous recording of elastically scattered protons from the target material with an NaI scintillation counter placed in the scattering chamber at 90° .

The relative (p, t) to $(p, {}^3\text{He})$ cross sections have an estimated uncertainty of less than 10% and were measured during the same experimental run, with the same configuration of target, beam, and detector system. The absolute cross sections were obtained by normalization to elastic scattering of protons on ${}^{33}\text{S}$ measured between 25° and 50° under identical experimental conditions. The measured elastic scattering cross sections were assumed to have the values calculated in the optical model using the parameters of Becchetti and Greenlees.⁵ The accuracy of the absolute cross sections thus determined is estimated to be about $\pm 20\%$.

Figure 1 shows spectra for ${}^{33}\text{S}(p, t){}^{31}\text{S}$ (upper half) and ${}^{33}\text{S}(p, {}^3\text{He}){}^{31}\text{P}$ (lower half) taken at the laboratory angle of 24° . Levels up to 7.2 and 7.6 MeV, respectively, were observed. Contaminant groups are hatched. The spectra were analyzed by the peak fitting program AUTOFIT.⁶

Mechanism of the $^{26}\text{Mg}(^{18}\text{O}, ^{16}\text{O})^{28}\text{Mg}$ reaction at $E_{^{18}\text{O}} = 50$ MeV and the energy levels of ^{28}Mg

M. Bernas, M. Roy-Stephan, F. Pougheon, M. Langevin, G. Rotbard, and P. Roussel
Institut de Physique Nucléaire, 91406 Orsay, France

J. P. LeFèvre, M. C. Lemaire, and K. S. Low
Département de Physique Nucléaire, CEN Saclay, BP No. 2, 91190 Gif-sur-Yvette, France

B. H. Wildenthal
Institut de Physique Nucléaire, 91406 Orsay, France
and Cyclotron Laboratory, Michigan State University, East Lansing, Michigan 48824
(Received 10 July 1978; revised manuscript received 6 February 1979)

The reaction $^{26}\text{Mg}(^{18}\text{O}, ^{16}\text{O})^{28}\text{Mg}$ has been studied at a bombarding energy of 50 MeV between laboratory angles of 4° and 17° . The differential cross sections of the lowest four states of ^{28}Mg have been compared to exact finite-range calculations in the distorted-wave Born approximation and coupled-channels Born approximation formulations. The reaction-mechanism calculations employed wave functions for the initial and final nuclear states which were generated in shell-model calculations carried out in the full $d_{5/2}$ - $s_{1/2}$ - $d_{3/2}$ basis space. The relative importance of one-step and two-step processes in the population of the different final states is evaluated and the effectiveness of current reaction theories in accounting for phenomena such as are exemplified by the present data is discussed.

[NUCLEAR REACTIONS $^{26}\text{Mg}(^{18}\text{O}, ^{16}\text{O})^{28}\text{Mg}$; enriched target, $E = 50$ MeV, measured $\sigma(\theta)$, microscopic DWBA and CCBA analysis with shell-model wave functions; deduced levels of ^{28}Mg .]

I. INTRODUCTION

We have studied the $^{26}\text{Mg}(^{18}\text{O}, ^{16}\text{O})^{28}\text{Mg}$ reaction with the aim of obtaining additional information about the level structure of ^{28}Mg , about which relatively little is known,¹⁻³ and of further elucidating the mechanism of heavy-ion two-nucleon transfer reactions, in particular the role of coupling between the inelastic-scattering and two-nucleon-transfer processes. In this report we present the results of analyzing the transitions to the lowest few states of ^{28}Mg with distorted-wave Born-approximation (DWBA) and coupled-channels Born-approximation (CCBA) calculations based on shell-model wave functions, together with results for the excitation energies and differential cross sections of the high-lying excited states which are strongly populated in this reaction.

The competition between the single-step transfer of a two-nucleon cluster from the target ground state to a given residual level and two-step processes connecting these same two levels which involve inelastic excitation of an intermediate state in either the target or residual nucleus (either before or after the transfer of the two-nucleon cluster) has been found to be significant in a variety of contexts. Studies have been carried out with targets in the light,^{4,5} medium⁶⁻⁹ and heavy regions^{10,11} and with both light-ion and heavy-ion

beams. When heavy-ion beams are utilized, the inelastic excitation of the projectile, such as ^{18}O in the present case, can also play a role.^{7,8,12} The present study is the first to combine a heavy-ion initiated reaction with the sort of detailed shell-model wave functions typically available only for lighter ($A \leq 40$) nuclei.

The study of the stripping of two neutrons onto ^{28}Mg to form states of ^{28}Mg offers a particularly clear avenue into the delineation of the relative importance of single-step and multiple-step reaction processes. This arises from the quasiclosure of the $d_{5/2}$ neutron orbit in the ^{28}Mg ground state, the wave function of which has as its leading term (relative to the ^{16}O core) $[d_{5/2}^v]_{J=0}^6 [d_{5/2}^\pi]_{J=0}^4$. The ground state of ^{28}Mg , which can similarly be approximated as $[d_{5/2}^v]_{J=0}^6 [s_{1/2}^v]_{J=0}^2 [d_{5/2}^\pi]_{J=0}^4$, can be directly populated by the addition of two neutrons in the $s_{1/2}$ orbit coupled to $J=0$. (More realistically, of course, the spread of the wave function over the adjacent shell-model orbits means that the actual transfer involves $J=0$ pairs of neutrons in each of the $d_{5/2}$, $s_{1/2}$, and $d_{3/2}$ orbits, insofar as the explicit theoretical wave functions utilized here are concerned, and even beyond that in nature. The simple point to be made is just that the "ground state to ground state" transition is "allowed.")

The dominant term of the wave function of the lowest 2^+ level of ^{28}Mg should be $[d_{5/2}^v]_{J=0}^6 [s_{1/2}^v]_{J=0}^2$

SEARCH FOR PARITY MIXING IN THE ^{93}Tc $\frac{17}{2}$ ISOMER: MEASUREMENTS OF PARTIAL γ -DECAY WIDTHS

B. A. BROWN †

Cyclotron Laboratory, Michigan State University, East Lansing, Michigan 48824, USA

and

O. HÄUSSER, T. FAESTERMANN ††, D. WARD, H. R. ANDREWS and D. HORN †††

*Atomic Energy of Canada Limited, Chalk River Nuclear Laboratories, Chalk River, Ontario,
Canada K0J 1J0*

Received 19 April 1978

Abstract: The angular distributions and linear polarizations of γ -rays emitted by the $\tau = 15 \mu\text{s}$ $\frac{17}{2}^-$ isomer in ^{93}Tc have been determined. The results imply upper limits of $\leq 6\%$ for the parity-violating E2 component in the 750.78 keV $\frac{17}{2}^- \rightarrow \frac{13}{2}^+$ transition and of ≤ 0.06 eV for the parity-violating matrix element, $|\langle \frac{17}{2}^+ | H_{p.v.} | \frac{17}{2}^- \rangle|$. The $\frac{17}{2}^- \rightarrow \frac{17}{2}^+$ level spacing was determined to be 0.30 ± 0.03 keV and the corresponding E1 branch was found to be $\leq 6\%$ of the $\frac{17}{2}^- \rightarrow \frac{13}{2}^+$ branch.

NUCLEAR REACTIONS $^{65}\text{Cu}(^{32}\text{S}, 2n2p)$, $E = 120$ MeV; measured $\gamma(\theta)$, linear polarization of delayed γ -rays. ^{93}Tc deduced levels, γ -branching, δ , limit on parity-violating E2 component in $\frac{17}{2}^- \rightarrow \frac{13}{2}^+$ transition. Enriched target, pulsed beam.

1. Introduction

In the last ten years there has been tremendous theoretical progress in the development of unified models for the weak and electromagnetic interactions by Weinberg and others ¹). The models have successfully predicted the existence of weak neutral currents, but the predicted parity-violating (p.v.) aspects of the weak neutral currents remain to be verified. Measurements of p.v. admixtures in nuclear levels provide a means of testing the purely hadronic part of the weak currents if the complexities associated with the strong interaction can be taken into account ²). The situation would be particularly promising if the most important term is associated with charged pion exchange between nucleons; in this case the calculations are relatively straightforward and the existence of p.v. weak neutral currents are predicted to lead to a large enhancement over the calculation with charged currents alone ³).

† Present address: Nuclear Physics Laboratory, Oxford, England.

†† NRCC Postdoctoral Fellow. Present address: Technische Universität, Munich, W. Germany.

††† NRCC Postdoctoral Fellow.

ROLE OF THE RMS RADIUS IN DWBA CALCULATIONS OF THE (p, d) REACTION †

A. MOALEM

Physics Department, Ben Gurion University, Beer Sheva, Israel

and

Département de Physique Nucléaire, CEN Saclay, BP 2, 91190 Gif-sur-Yvette, France

J. F. A. VAN HIENEN **

Michigan State University, East Lansing, Michigan 48824

and

E. KASHY

Michigan State University, East Lansing, Michigan 48824

and

Institut de Physique Nucléaire, Orsay 91, France

Received 27 February 1978

(Revised 19 June 1978)

Abstract: The single-neutron pick-up reaction cross sections appear to be better correlated with the rms radius of the neutron orbit rather than with r_0 , the radius parameter of the single-particle Woods-Saxon well. Form factors which correspond to particles bound by the experimental separation energies and which have rms radii for the $2s_{1/2}$, $1d_{3/2}$ and $1f_{7/2}$ orbits obtained from Coulomb energy shifts, lead to spectroscopic factors and S_p/S_c ratios for the $^{46,48,50}\text{Ti}(p, d)$ reactions which are in a much better agreement with theoretical expectations than those obtained with constant r_0 .

1. Introduction

It is a common procedure in DWBA analyses to calculate radial form factors characteristic of single-nucleon states in a Woods-Saxon (WS) well of radius $R = r_0 A^{1/3}$. A radius parameter $r_0 \approx 1.25$ fm, a diffuseness $a = 0.65$ fm and a spin-orbit term $\lambda = 25$ are often used, while the potential depth is adjusted to reproduce the experimental values of binding energies, i.e. the nuclear separation energies. It has been indicated by Friedman *et al.* ¹⁾ that the geometrical parameters of the potential well are not uniquely determined and hence that the sub-Coulomb stripping ²⁾ cross sections calculated with these form factors are not reliable. In particular, the calculated

† Research supported in part by the US National Science Foundation.

** Fellow of the Niels Stensen Foundation, the Netherlands.

Present address: Natuurkundig Laboratorium der Vrije Universiteit, Amsterdam, The Netherlands.

A STUDY OF THE $^{54}\text{Fe}(p, d)^{53}\text{Fe}$ REACTION AT 40 MeVT. SUEHIRO[†], J. E. FINCK and J. A. NOLEN, Jr.Cyclotron Laboratory, Michigan State University, East Lansing, Michigan 48824^{**}

Received 29 May 1978

(Revised 14 August 1978)

Abstract: The $^{54}\text{Fe}(p, d)^{53}\text{Fe}$ reaction was studied using 40 MeV protons with a split-pole magnetic spectrograph. A total of 53 states were observed up to an excitation energy of 7.364 MeV in ^{53}Fe . At least 29 of these states have not been previously reported. Angular distributions were measured from 6° to 90° for transitions to 35 of these states, and were analysed with distorted-wave Born approximation calculations. Excitation energies, transferred l -values, spectroscopic factors and the implied J^π values are given. Difficulties encountered in obtaining a reliable set of spectroscopic factors are discussed in relation to various prescriptions in the DWBA calculations, and to the one-nucleon transfer sum rule.

E NUCLEAR REACTION $^{54}\text{Fe}(p, d)$, $E = 40.16$ MeV; measured $\sigma(\theta, E_p)$. ^{53}Fe deduced levels, l , spectroscopic factors. ^{54}Fe enriched target.

1. Introduction

From the simplest shell-model point of view the nucleus ^{54}Fe has a closed $0f_{7/2}$ neutron shell and the two proton holes in the same orbit. The neutron pickup reaction is then expected to populate states of ^{53}Fe which arise from neutron holes in the closed neutron core. Strengths of population of states arising from shell-model orbits above the $0f_{7/2}$ orbit provide a measure of the degree of shell closure at $N = 28$. For this reason neutron pickup reactions have been extensively investigated using ($^3\text{He}, \alpha$) and (d, t) reactions¹⁻³ as well as the (p, d) reaction⁴⁻⁶ on ^{54}Fe . Among these the (p, d) reaction has been regarded as yielding the most reliable absolute spectroscopic factors, despite the large negative Q -value. Sherr *et al.*⁵) identified levels in ^{53}Fe by the (p, d) reaction at 28 MeV and made spin-parity assignments to four excited states below 4.24 MeV excitation. Nelson *et al.*⁶) studied the same reaction at 29 MeV, identifying seven levels below 2.840 MeV, and giving transferred l -values and spectroscopic factors for five of them. They also determined accurate excitation energies by use of the $^{50}\text{Cr}(\alpha, n\gamma)$ reaction at several bombarding energies. The ($^3\text{He}, \alpha$) reaction was studied by Borlin¹) at 33 MeV

[†] On leave from Tohoku Institute of Technology, Nagamachi, Koeji-19, Sendai 982 Japan.^{**} Research supported by the US National Science Foundation.

STUDY OF ^{60}Zn AND ^{61}Zn

D. J. WEBER, G. M. CRAWLEY, W. BENENSON, E. KASHY and H. NANN

Cyclotron Laboratory and Physics Department, Michigan State University, East Lansing, MI 48824

Received 6 December 1977

(Revised 2 August 1978)

Abstract: The (^{12}C , ^{10}Be) and (^{12}C , ^9Be) reactions on ^{58}Ni were studied at 77 MeV. New levels were determined for both residual nuclei, ^{60}Zn and ^{61}Zn . For ^{61}Zn , levels and a new ground state mass were also measured with the $^{64}\text{Zn}(^3\text{He}, ^6\text{He})$ reaction. A mass excess for ^{61}Zn of -56333 ± 23 keV was obtained. Angular distributions for the ^{12}C induced reactions are compared with finite range DWBA calculations and found to be insensitive to L - and J -transfer.

NUCLEAR REACTIONS $^{58}\text{Ni}(^{12}\text{C}, ^{10}\text{Be})$, $^{58}\text{Ni}(^{12}\text{C}, ^9\text{Be})$, $E = 77$ MeV; measured $(E_{^{10}\text{Be}}, \theta)$, $(E_{^9\text{Be}}, \theta)$. ^{60}Zn , ^{61}Zn deduced levels. $^{64}\text{Zn}(^3\text{He}, ^6\text{He})$, $E = 70$ MeV; measured σ ; deduced Q . ^{61}Zn deduced mass excess levels. Enriched targets. ATOMIC MASS ^{61}Zn .

1. Introduction

Little is known about the most proton rich zinc isotopes ^{60}Zn and ^{61}Zn . The nucleus ^{60}Zn has been studied previously by the $^{58}\text{Ni}(^3\text{He}, n)$ reaction with an energy resolution between 300 and 500 keV FWHM [refs. 1–3]) and by a ($^3\text{He}, n\gamma$) experiment 4) which measured the energies of four excited states up to 4.2 MeV of excitation with high precision. In the case of ^{61}Zn , earlier mass excess measurements from β -decay 5) and from the $^{58}\text{Ni}(^4\text{He}, n)$ threshold 6) were imprecise and in poor agreement with each other. Recently, precise measurements of the mass and energy levels of ^{61}Zn by the reaction $^{58}\text{Ni}(^6\text{Li}, t)$ have been reported 7). On the theoretical side, shell model calculations of the spectra of these zinc isotopes have been performed by Van Hienen, Chung and Wildenthal 8), and provide in part the incentive for the present work.

Both ^{60}Zn and ^{61}Zn can be studied using heavy ion beams. Since heavy ion transfer reactions favour final states of higher spin than do the ($^3\text{He}, n$) and ($^4\text{He}, n$) reactions, they tend to complement rather than reproduce the results of experiments involving those reactions. For the case of $^{58}\text{Ni}(^{12}\text{C}, ^{10}\text{Be})^{60}\text{Zn}$ at 77 MeV, a simple semiclassical picture 9) shows that the favoured L -transfer for the low excitation region of the spectrum is about 5. Thus, low spin states which are observed preferentially in ($^3\text{He}, n$) at forward angles may be quite weak in the present experiment. Besides the new information one can gain on the levels of ^{60}Zn and ^{61}Zn , the reaction me-

HIGH-SPIN ROTATIONAL LEVELS IN ^{178}W POPULATED IN THE $^{177}\text{Hf}(\alpha, 3n\gamma)$ REACTION [†]

C. L. DORS ^{**}, F. M. BERNTHAL, T. L. KHOO ^{***} and C. H. KING [‡]

*Departments of Chemistry and Physics and Cyclotron Laboratory, Michigan State University,
East Lansing, Michigan 48824*

and

J. BORGGREEN and G. SLETTEN

Niels Bohr Institute, Tandem Accelerator Laboratory, Risø, 4000 Roskilde, Denmark

Received 29 August 1978

Abstract: High-spin rotational levels in ^{178}W were populated in the $^{177}\text{Hf}(\alpha, 3n\gamma)$ reaction. The yrast sequence of states is identified to spin 16 and is contrasted with similar data for ^{180}W and ^{182}W . Two probable two quasi-neutron bands with $K^\pi = 6^+$ and 7^- are characterized from derived g_K values and decay patterns. The $K^\pi = 2^-$ octupole band is identified to spin 13, and the higher-spin members of the lowest $K^\pi = 0^+$ band are placed. A 35 ns isomer is identified at 3528 keV.

NUCLEAR REACTIONS $^{177}\text{Hf}(\alpha, 3n)$, $E = 38$ MeV; measured E_α , $I_\alpha(\theta)$, E_γ versus E_α , $\gamma\text{-}\gamma$ - t coin, $\alpha\gamma$ -delay. ^{178}W deduced levels, J , π , K , $T_{1/2}$, multipolarities. Ge(Li) detectors. Enriched target.

1. Introduction

The spectroscopy of the yrast and near-yrast sequence of states in deformed nuclei has been a subject of some interest for the past several years. Such yrast-line studies have provided a wealth of information on the backbending phenomenon in the ground bands of deformed even- A nuclei, while complementary data from odd- A rotational bands have provided insight into the causes of backbending. The general understanding has emerged that backbending is primarily a manifestation of rotation-alignment (RA) effects in nuclei at high angular momentum. Nevertheless, the details of the RA mechanism are still poorly understood, particularly near the large- A limit of the rare-earth region of deformation ¹⁾.

[†] Research supported in part by the US National Science Foundation.

^{**} Present address: Chemistry Department, Purdue University, West Lafayette, Indiana 47907

^{***} Present address: Physics Division, Argonne National Laboratory, Argonne, Illinois 60439.

[‡] Present address: Nuclear Science Division, Lawrence Berkeley Laboratory, Berkeley, California 84720.

STUDY OF THE $^{10}\text{Be}(d, p)^{11}\text{Be}$ REACTION AT 25 MeV †

B. ZWIEGLINSKI ††, W. BENENSON and R. G. H. ROBERTSON

Cyclotron Laboratory and Department of Physics, Michigan State University, East Lansing, Michigan 48824

and

W. R. COKER *

Department of Physics, University of Texas at Austin, Austin, Texas 78712

Received 18 July 1978

(Revised 25 September 1978)

Abstract: The distribution of the single-neutron strength up to an excitation energy $E_x = 7.0$ MeV in ^{11}Be was investigated with the $^{10}\text{Be}(d, p)^{11}\text{Be}$ reaction at $E_d = 25$ MeV. The $\frac{1}{2}^+$, g.s., $\frac{1}{2}^-$, 0.320 MeV and 1.785 MeV states are found to be excited with significant strength. The angular distribution for the 1.785 MeV state is typified by an orbital angular momentum transfer $l_p = 2$. This together with other available data indicate that its spin is $J^\pi = (\frac{3}{2})^+$. The spectroscopic factors for these three states are compared to the shell-model calculations of Teeters and Kurath and of Cohen and Kurath.

E NUCLEAR REACTIONS $^{10}\text{Be}(d, p)$, $E = 25$ MeV; measured $\sigma(\theta)$; deduced spectroscopic factors. Reactor-produced ^{10}Be target.

1. Introduction

Due to the work of Kurath and collaborators ^{1,2)}, shell-model wave functions are presently available for both positive and negative parity states in $A = 11$ and $A = 13$ nuclei. The wave functions for the negative parity states were obtained by Cohen and Kurath ¹⁾ in 1965. An important step on the way to the wave functions for the positive parity states was the derivation ³⁾ of a particle-hole interaction which is capable of reproducing the A -dependence of the $2s_{\frac{1}{2}}-1d_{\frac{3}{2}}$ splitting in the $11 \leq A \leq 17$ nuclei. The ordering of the $1d_{\frac{3}{2}}$ and $2s_{\frac{1}{2}}$ orbits changes with decreasing mass in this mass range, with the $2s_{\frac{1}{2}}$ orbit lying lower in energy below mass number $A = 15$. This particle-hole interaction was subsequently used by Teeters and Kurath ²⁾ to calculate the wave functions for the positive parity states in the $A = 11$ and $A = 13$ nuclei. A full vector space compatible with the $(1s)^3(1p)^{A-3}$ and $(1s)^4(1p)^{A-5}(2s, 1d)$

† Work supported by the US National Science Foundation under Grant No. PHY 78-01684.

†† On leave from the Institute of Nuclear Research, Warsaw, Poland.

* Research supported in part by the US Department of Energy.

CHARGE-DEPENDENT TWO-BODY INTERACTIONS DEDUCED FROM DISPLACEMENT ENERGIES IN THE $1f_{7/2}$ SHELL[†]

B. A. BROWN^{**}

Cyclotron Laboratory, Michigan State University, East Lansing, Michigan 48824

and

R. SHERR

Joseph Henry Laboratories, Princeton University, Princeton, New Jersey 08540

Received 27 October 1978

(Revised 2 February 1979)

Abstract: The $f_{7/2}$ shell model is used to relate displacement energies in the region $A = 41$ –55 to a single-particle displacement energy and the differences between the proton-proton, proton-neutron, and neutron-neutron two-body matrix elements for $J = 0, 2, 4$ and 6 . We find that the displacement energies for essentially all measured states (about 60) can be calculated to within an rms deviation of 12 keV by using a fixed set of these parameters. A few discrepancies such as for the 0^+ and 2^+ states in $A = 42$ can be due to large admixtures outside $f_{7/2}$ configurations. The deduced two-body matrix elements are compared with previous results for the $d_{5/2} s_{1/2}$ and $d_{3/2}$ shells. The empirical results are compared with calculations of the Coulomb two-body matrix elements assuming j^2 configurations. The empirical pp-nn matrix elements are anomalous relative to these simple calculations. The size of the anomaly for the $2J+1$ weighted average of the pp-nn interactions in the $1f_{7/2}$ shell is about the same as that deduced from the single-particle nuclei by Nolen and Schiffer; the J -dependence of the anomaly is very irregular. The empirical pn-nn matrix elements are consistent with zero except in the case of $J = 0$. The anomalies in both the pp-nn and pn-nn interactions may be due to configuration mixing and/or a charge dependence in the nucleon-nucleon interaction. The importance of the mass dependence in $\hbar\omega$ for rms radii and Coulomb shifts is discussed. The displacement energies for proton rich $f_{7/2}$ nuclei are predicted and isospin-mixing matrix elements are calculated. Relations between the exact calculation and the generalized-seniority approximation are discussed.

1. Introduction

The displacement energies of analogue states provide an important test of the nuclear interactions. If we assume that the strong interaction is charge invariant then the displacement energies give direct information on the many-body structure of the nuclear wave functions since the Coulomb interaction is well known. Alternatively, if the nuclear structure is known then the displacement energies provide

[†] Research supported in part by the US National Science Foundation.

^{**} Present address: University of Oxford, Nuclear Physics Laboratory, Keble Road, Oxford OX1 3RH, England.

LETTERS TO THE EDITOR

FAST RESOLUTION OPTIMIZATION IN A MAGNETIC SPECTROGRAPH*

E. KASHY, P. S. MILLER and J. A. NOLEN, Jr.

Cyclotron Laboratory, Michigan State University, East Lansing, Michigan 48824, U.S.A.

Received 9 June 1978

A technique for quickly tuning accelerator and beam optics parameters to obtain high resolution in a magnetic spectrograph is described.

This letter reports a beam tuning technique which has applications in accelerator, beam transport, and magnetic spectrograph diagnostics. In an earlier paper, Blosser et al.¹⁾ described a dispersion-matching system and a tuning method for high resolution charged particle spectroscopy. The present work uses the same ideas, except that the information required for tuning is derived from direct observation of the beam image size and shape in the spectrograph focal plane using an optical system with high magnification.

Briefly, the tuning method described by Blosser et al.¹⁾ consists of minimizing the line width for elastic scattering of charged particles from a thin target, with the spectrograph at a small angle where there is a large count rate. The particles are

observed in a detecting device from which the experimenter gets a one-dimensional parameter, the line width in the focal plane of the magnetic spectrograph. The various bending magnets, quadrupoles, and sextupole are adjusted to minimize the line width. Since extremely narrow lines have been achieved, it is essential that during the tuning, some feedback system maintains the elastically scattered particles at the same position on the focal plane. A computer controlled feedback has been installed for that purpose, and if during the adjustments the line is displaced due to small misalignments, the spectrograph magnetic field is changed to bring it back on the width-sensing detector. Thus the resolution-optimizing procedure can be rather time consuming. Indeed, excellent results have been obtained²⁾, e.g., 1.5 keV fwhm for elastic scattering of 35 MeV protons from a

* Work supported by the U.S. National Science Foundation.

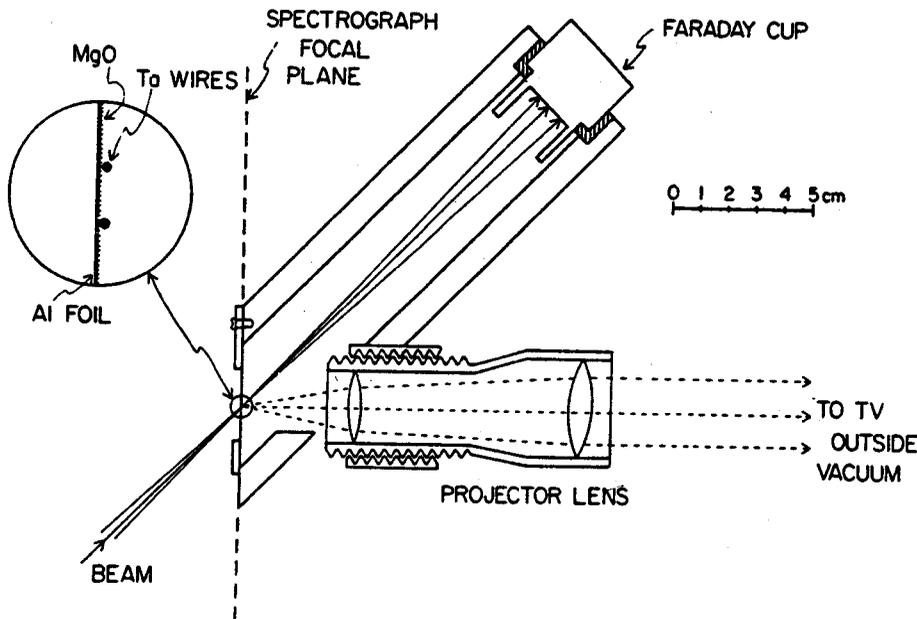


Fig. 1. Viewing apparatus positioned in the spectrograph focal plane. Light from the lens traverses a plastic window before entering the television camera lens. The two vertical wires in the insert, which are 25 μm in diameter and are separated by 2 mm, serve to calibrate the width and relative position of the beam image.

AN EASILY PREPARED SCINTILLATOR FOR VIEWING ACCELERATOR BEAM SPOTS*

J. A. NOLEN, Jr.

Cyclotron Laboratory, Michigan State University, East Lansing, Michigan 48824, U.S.A.

Received 9 June 1978

The preparation of thin MgO scintillators and some of their applications for beam viewing are described.

This note describes the preparation of thin MgO layers which are useful for viewing beam spots of light and heavy-ion beams. For viewing relatively intense or highly ionizing beams, such as several microamperes of 70 MeV ^3He ions, these scintillators often have advantages over others such as quartz, zinc sulfide, BeO, or thin plastic scintillators.

The main advantages of MgO scintillators are that they are very easy to prepare, can be made in thin layers on thin backings, are relatively insensitive so that the light output does not saturate even with fairly intense beams, and are relatively resistant to radiation damage compared with other more commonly used scintillators. The MgO scintillators described here have been used for several years in beam focussing at the MSU Cyclotron, but recently they have found additional application in the direct viewing of very narrow beam images in the focal plane of a magnetic spectrograph¹⁾ and also as a water-cooled fast scintillator on a phase measuring probe²⁾ at the MSU cyclotron.

A thin layer of MgO can be deposited on a thin backing by burning a strip of Mg metal foil in air and collecting the white "smoke" on the backing foil. Burning about 0.1 g of Mg in the form of a strip about 6 cm long \times 3 mm wide \times 0.1 mm thick and holding the burning Mg about 5–10 cm below a horizontally mounted backing foil produces MgO oxide layers in a useful thickness range. The Mg foil is easily ignited with the flame of a propane torch. Backings of household aluminum foil, i.e. 6–12 μm in thickness, mounted on standard target frames are convenient for most purposes. A good thickness of the MgO layer for

TV viewing of beam spots is obtained when the MgO layer just becomes opaque, i.e. the backing is not visible through the white MgO film. Thinner layers are probably also useful for highly ionizing very intense beams, but much thicker layers tend to flake off of the backing foils. Fig. 1 shows a beam image on a MgO scintillator prepared as described here.

The scintillators used on the internal phase measuring probe²⁾ of the cyclotron are prepared as described above except much thinner layers, i.e. barely visible by eye, are used and they are depos-

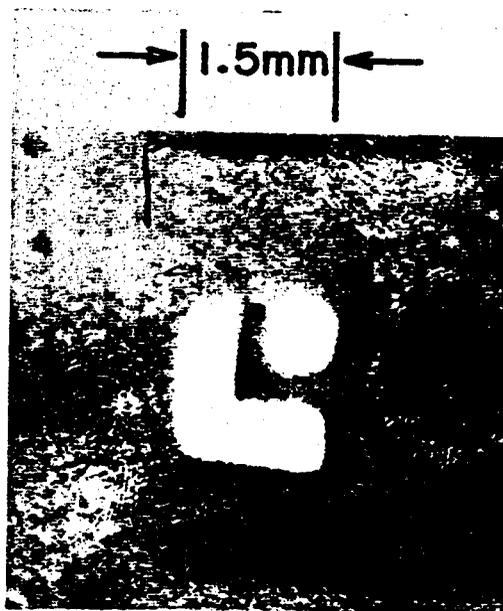


Fig. 1. The image of a proton beam (about $1 \mu\text{A}$ at 35 MeV) on a MgO scintillator at the target position of a magnetic spectrograph. The beam was passed through a Ta aperture of known dimensions upstream from the target and imaged via a quadrupole triplet to form the image shown. This image was photographed from a TV monitor screen. The image size on target was 1.5 mm \times 1.5 mm.

* Research supported by U.S. National Science Foundation.

TAPPED DELAY LINE FOCAL PLANE DETECTORS*

R. G. MARKHAM**

Cyclotron Laboratory, Michigan State University, East Lansing, MI 48824, U.S.A.

The use of commercially available tapped delay lines in focal plane detectors is illustrated by four examples. These lines are small and rugged. They offer design flexibility, high resolution and dynamic range, moderately fast readout and simultaneous event suppression.

1. Introduction

Many factors affect the design of position sensitive detectors for magnetic spectrograph focal planes. Line widths as small as $50\ \mu\text{m}$ have occasionally to be resolved and lengths as long as 2 m sometimes need to be covered. In addition to detecting and locating particles one always must be able to identify them, whether it be to tell a proton from a deuteron or ^{25}Mg from ^{24}Mg . Identification may require a fast time measurement, precise energy loss or energy measurement, or all of them. Additionally one also needs position in the orthogonal direction and angles of incidence if ray tracing or aberration corrections are required.

Obviously no single detector can be made which accomplishes all this. One must use a variety of detection schemes and designs each intended to measure a particular set of parameters using the techniques best suited to the measurements to be made. Thus an additional consideration is that detectors be transparent so that they may be followed by successive ones. It also follows that the most popular readout scheme will be the one that is most adaptable and least restrictive while maintaining a high level of performance.

We at Michigan State University have found that various commercially available tapped delay lines allow detector designs that have many of the ideal properties mentioned above and are particularly adaptable to a wide variety of uses. In the following I will describe four uses of these delay lines which separately illustrate particular features and advantages they possess. In doing so, I will borrow heavily from the work of ref. 1, the unpublished work of my colleagues, and a project of mine which is in the developmental stage.

* Research supported in part by the U.S. National Science Foundation.

** Present address: Xerox Corporation, W-200, Webster, New York, 14580 NY, U.S.A.

2. The inclined stripe counter

2.1. INTRODUCTION

The most widely used active detector in the focal plane of the popular Enge split-pole spectrograph is perhaps the resistive-anode proportional counter^{2,4}) using either charge division or rise-time effects to locate the event. Although these detectors generally do not give submillimeter resolution, they are preferred because of their low cost, simplicity and ability to transmit the detected particles to backing detectors which serve to reduce background events and to improve the particle identification. Significantly better resolution has been obtained in detectors where the position is determined by relative timing of signals at the ends of a helically wound delay line which serves as the cathode of a proportional counter⁵). This device has good position resolution but is difficult to back with a second detector and is very bulky. A general feature of both types of counters is the steady deterioration of resolution as one goes to higher energy, lighter ions.

Thus, it has been our objective to design a counter which provides high resolution even for lightly ionizing particles, while retaining the virtues of the resistive anode devices. In section 2, I discuss some of the processes taking place in the detection and localization of a particle in a proportional counter. In later sections the design and performance of a detector which meets the desired objective will be briefly described and theoretical limits for the position resolution will be presented and compared with the results obtained. Since this detector is fully described in ref. 1, I shall leave out many details in the following.

2.2. POSITION RESOLUTION

2.2.1. Effects of energy-loss fluctuations

The resistive anode counters²) are capable of position resolution better than 0.3 (0.05) mm for highly

B. H. Wildenthal^{*†}

Gesellschaft für Schwerionenforschung, D-6100 Darmstadt

and

*Cyclotron Laboratory***, Michigan State University
East Lansing, Michigan 48824

ANALYSIS OF NUCLEAR SPECTROSCOPIC DATA WITH THE SHELL MODEL^{***)}

The genesis, evolution and consequences of some shell model calculations for $A = 18-38$ nuclei are described. Emphasis is given to the relationships between theoretical matrix elements and the reduced values from experimental measurements, with the aim of clarifying the important aspects of comparisons between theoretical and experimental results.

1. Introduction

Our subject here is the relationship between the conventional nuclear shell model and the various types of spectroscopic data obtained in current experimental studies of light nuclei. Our approach is first to discuss theoretical aspects, then relationships between experimentally measured and calculated numbers. Our treatment of shell model theory consists of some elementary and general introductory remarks and a detailed description of some specific calculations which shall be systematically use as examples. The main body of a comprehensive theoretical discussion—foundations, formal and computational techniques, and a survey of the existing research literature — is omitted. Some compensatory information is available in Refs. 1-10. Our treatment of experimental spectroscopy is similarly bifurcated into some rather casual observations on general classes of experiments and some detailed presentations of selected examples of data. We concentrate upon the conclusions which follow from a thorough analysis of experimental data with existing theoretical tools. As such, one of the two principal aims of this presentation is to convey a comprehension of how extensive is the body of data which can be subsumed into a unified shell model approach and what is the degree of accuracy to which such an approach reproduces the results of experiment. The other goal is hopefully to remove some of the mystery which often attends comparisons of experimental

^{*}) John Simon Guggenheim Memorial Foundation Fellow, 1977

[†] permanent address, Cyclotron Laboratory, M.S.U., E. Lansing, Mi., 48824

^{**}) research supported in part by the U.S. National Science Foundation

^{***}) Invited talk at the tenth Summer School of Nuclear Physics, August 30-September 1, 1977, Mikołajki, Poland.

Initial Organic Products of Assimilation of [^{13}N]Ammonium and [^{13}N]Nitrate by Tobacco Cells Cultured on Different Sources of Nitrogen¹

Received for publication January 23, 1978 and in revised form April 11, 1978

THOMAS A. SKOKUT,² C. PETER WOLK, JOSEPH THOMAS,³ JOHN C. MEEKS⁴ AND PAUL W. SHAFFER
MSU-ERDA Plant Research Laboratory

W.-S. CHIEN

Cyclotron Laboratory and Department of Physics, Michigan State University, East Lansing, Michigan 48824

ABSTRACT

Glutamine is the first major organic product of assimilation of $^{13}\text{NH}_4^+$ by tobacco (*Nicotiana tabacum* L. cv. Xanthi) cells cultured on nitrate, urea, or ammonium succinate as the sole source of nitrogen, and of $^{13}\text{NO}_3^-$ by tobacco cells cultured on nitrate. The percentage of organic ^{13}N in glutamate, and subsequently, alanine, increases with increasing periods of assimilation. $^{13}\text{NO}_3^-$, used for the first time in a study of assimilation of nitrogen, was purified by new preparative techniques. During pulse-chase experiments, there is a decrease in the percentage of ^{13}N in glutamine, and a concomitant increase in the percentage of ^{13}N in glutamate and alanine. Methionine sulfoximine inhibits the incorporation of ^{13}N from $^{13}\text{NH}_4^+$ into glutamine more extensively than it inhibits the incorporation of ^{13}N into glutamate, with cells grown on any of the three sources of nitrogen. Azaserine inhibits glutamate synthesis extensively when $^{13}\text{NH}_4^+$ is fed to cells cultured on nitrate. These results indicate that the major route for assimilation of $^{13}\text{NH}_4^+$ is the glutamine synthetase-glutamate synthase pathway, and that glutamate dehydrogenase also plays a role, but a minor one. Methionine sulfoximine inhibits the incorporation of ^{13}N from $^{13}\text{NO}_3^-$ into glutamate more strongly than it inhibits the incorporation of ^{13}N into glutamine, suggesting that the assimilation of $^{13}\text{NH}_4^+$ derived from $^{13}\text{NO}_3^-$ may be mediated solely by the glutamine synthetase-glutamate synthase pathway.

Ammonium assimilation in higher plants was long thought to begin with the synthesis of glutamate by glutamate dehydrogenase. There is now reason to believe that the major route for assimilation of ammonium may be the glutamine synthetase-glutamate synthase pathway (21). Evidence for the presence of this pathway in higher plants is largely based on enzymological studies and on studies performed with ^{15}N -labeled nitrogen. Glutamine synthetase has been found in several plant tissues (7, 22, 29) and was observed to be localized in the chloroplasts (12, 13, 23). A pyridine

nucleotide-dependent glutamate synthase has been found in extracts of tissue cultures from six different species (5, 6) and a ferredoxin-dependent glutamate synthase has been described from leaf tissue (15). However, the detection of these activities in plant tissues does not prove that they have a substantial role in the assimilation of ammonium.

When $^{15}\text{NO}_3^-$, [^{15}N]amide glutamine, and [^{15}N]amino glutamate were fed separately to pea leaves, ^{15}N appeared in free and protein-bound amino acids in similar proportions regardless of the labeled substrate applied (18). This observation was consistent with assimilation via the glutamine synthetase-glutamate synthase pathway because the ^{15}N would presumably have had to have passed sequentially through these compounds in order for the amino acids to become labeled in similar proportions. Studies done with a 10-hr feeding of $^{15}\text{NO}_3^-$ via the transpiration stream of cut shoots of *Datura* demonstrated that glutamine was the predominant recipient of photosynthetically reduced nitrogen in the leaf (16, 17). A kinetic study of the appearance of ^{15}N in soluble nitrogenous compounds in roots of rice seedlings supplied with $^{15}\text{NH}_4^+$ or $^{15}\text{NO}_3^-$ showed that glutamine was the most rapidly labeled compound, with concurrent but slower labeling of glutamic acid, aspartic acid, and alanine, in that order (32, 33). The shortest times for which the incorporation of label was tested were 5 min in the $^{15}\text{NO}_3^-$ studies and 15 min in the $^{15}\text{NH}_4^+$ studies. In a recent investigation, young pea leaves were supplied with $^{15}\text{NO}_3^-$ in the light and dark, and the incorporation of ^{15}N into various components of the leaves was followed (3). A large portion of the ^{15}N appeared in the amide group of glutamine and turned over rapidly. Glutamic acid and alanine also became labeled, although less than glutamine. Incorporation into aspartic acid, γ -aminobutyric acid, and homoserine was slower. The shortest period of labeling in these studies was 1 hr.

The demonstration of the presence of both glutamine synthetase and glutamate synthase in plants and the studies of the kinetics of labeling are consistent with an involvement of the glutamine synthetase-glutamate synthase pathway in the assimilation of ammonium by higher plants. However, a precursor-product relationship between the metabolites involved has not been established; it has not been tested whether the assimilatory pathway is dependent upon the nitrogen source used for growth; and there has been only one instance (1) where use has been made of inhibitors of the enzymes involved in the pathway, to test whether the labeling observed is dependent on those enzymes.

The use of $^{13}\text{NH}_4^+$ in studies of nitrogen metabolism in *Anabaena cylindrica* and other cyanobacteria has been reported (19, 25; Meeks *et al.*, unpublished observations). In this paper, we report on the initial products of assimilation of $^{13}\text{NH}_4^+$ by tobacco cells cultured with nitrate, urea, or ammonium succinate as the

¹ This work was supported by U.S. Energy Research and Development Administration Contract EY-76-C-02-1338 and by National Science Foundation Grants 74-01206 and 78-01684. This work is taken from a dissertation to be submitted to Michigan State University by T. A. S. in partial fulfillment of the requirements for the degree of Ph.D. in botany.

² Present address: Department of Biology, Washington University, St. Louis, Missouri 63130.

³ Present address: Biology and Agriculture Division, Bhabha Atomic Research Centre, Trombay, Bombay 400 085, India.

⁴ Present address: Department of Bacteriology, University of California, Davis, California 95616.

The Acetylene Inhibition Method for Short-term Measurement of Soil Denitrification and its Evaluation Using Nitrogen-13¹

M. SCOTT SMITH, MARY K. FIRESTONE, AND JAMES M. TIEDJE²

ABSTRACT

Acetylene was found to effectively inhibit the reduction of N₂O by anaerobic soils. With concentrations of C₂H₂ above 0.1 atm, added NO₃⁻ was quantitatively converted to N₂O, and added N₂O was reduced at an insignificant rate. Experiments with ¹³N demonstrated that at low soil nitrate concentrations at least 0.1 atm C₂H₂ was required for effective inhibition. Denitrification rates determined by ¹³N and by C₂H₂ inhibition methods correlated well, as did determinations of N₂O/(N₂ + N₂O). The methods also revealed that an acceleration in denitrification rate occurred within a few hours after soil was exposed to anaerobic conditions. The acetylene method was generally used to measure denitrification rates in soils incubated as anaerobic slurries, but was also used to determine rates for field moist aggregates incubated anaerobically and aerobically. When assayed as anaerobic slurries, initial denitrification rates ranged from 0.1 to 0.7 nmoles N gas · soil⁻¹ · min⁻¹ for the mineral soils examined. The denitrification rate in aerobic aggregates was approximately 1,000 times less, showing the strong inhibitory effect of O₂ on the indigenous denitrifying enzymes.

Additional Index Words: nitrous oxide, nitrogen losses, nitrogen transformations.

Smith, M. Scott, Mary K. Firestone, and James M. Tiedje. 1978. The acetylene inhibition method for short-term measurement of soil denitrification and its evaluation using nitrogen-13. *Soil Sci. Soc. Am. J.* 42:611-615.

THE INCREASED COST OF FIXED nitrogen and the possibility that soil-evolved N₂O may contribute to atmospheric ozone depletion (McElroy et al., 1976) have caused renewed interest in the process of denitrification. Despite a considerable mass of research on denitrification, reliable values for rates of N₂ and N₂O production in field

soils are lacking. Due to limited sensitivity, previous methods have required extensive amendment of soils and/or long term incubation. Although these methods have elucidated the basic controlling factors, the dynamics of denitrification and the quantitative effects of environmental or management parameters on natural soils are largely unknown.

The inhibition of N₂O reductase by acetylene in pure culture was reported by Yoshinari and Knowles (1976) and by Balderston, et al. (1976). It is now widely accepted that N₂O is an obligatory, and probably freely diffusible intermediate in the denitrification pathway (Payne, 1973; St. John and Hollocher, 1977). Therefore, one would expect the quantity of N₂O produced by C₂H₂-inhibited microorganisms to be a direct measure of the total gaseous N produced without inhibition. If N₂O is the sole denitrification product, analysis is greatly simplified since N₂O, unlike N₂, is a minor atmospheric constituent (approximately 300 ppb) and can be assayed by sensitive gas chromatographic detectors. The successful application of this method to soil denitrification studies has been reported by Yoshinari, et al. (1977).

In this paper we have used gas chromatography and ¹³NO₃⁻ to evaluate the acetylene inhibition technique in soils and have identified the conditions and soil types for which this method is valid and for which blockage of N₂O reductase is complete. The radioactive isotope, ¹³N, provides an extremely sensitive assay, with excellent temporal resolution, which can be used without alteration of native NO₃⁻ concentration.

MATERIALS AND METHODS

The soils used are described in Table 1. Soils were near field capacity when collected, and without drying, were passed through a 5-mm sieve and stored in sealed plastic bags at 2°C until used. The storage period varied from 1 day to 6 months. Soil slurries were used in most of the C₂H₂ inhibition assays.

¹Contribution from the Dept. of Crop and Soil Sciences and Dept. of Microbiology and Public Health, Michigan State Univ., East Lansing, MI 48824. Journal article no. 8280. of the Michigan Agric. Expt. Stn. Received 3 Oct. 1977. Approved 6 Mar. 1978.

²Research Assistants and Associate Professor, respectively.

Application of the semiclassical method to polarization

G. Bertsch (*)

Dept. of Physics and Cyclotron Laboratory, Michigan State University,
East Lansing, Michigan 48824, U.S.A.

and R. Schaeffer

Centre d'Etudes Nucléaires de Saclay,
B.P. n° 2, 91190 Gif sur Yvette, France

(Reçu le 16 août 1978, accepté le 4 octobre 1978)

Résumé. — Une formulation de la polarisation en diffusion élastique est établie à partir de l'approximation semi-classique. La polarisation s'exprime comme une somme de deux termes, l'un proportionnel à l'angle et l'autre proportionnel à la dérivée de la section efficace. Les amplitudes relatives de ces deux termes dépendent de la phase entre le potentiel spin-orbite et le potentiel réel. Ce résultat est comparé à des calculs quantiques dans différents cas. Bien que quantitativement peu précise, cette formulation reproduit de manière qualitative dans diverses conditions le comportement général de la polarisation.

Abstract. — A formula is derived for the polarization in elastic scattering, based on the semiclassical approximation. The polarization is given by the sum of two terms, one proportional to the angle and one proportional to the derivative of the cross section. The relative magnitudes of the terms depend on the relative phase of the spin orbit potential with respect to the real potential. This is compared with quantum calculations for several cases. While not quantitatively accurate, the formula reproduces the qualitative behaviour of the polarization under a broad range of conditions.

1. Introduction. — The qualitative behaviour of polarization in elastic scattering has long been obscure [1]. In the 1950's, semiclassical expressions were derived for polarization based on the Thomas form for the spin-orbit interaction [2, 3]. This yields a polarization that is proportional to scattering angle θ , when the central potential is imaginary. While the experimental data often shows a smoothly rising polarization with angle, the polarization often displays oscillations resembling the derivative of the elastic scattering cross section. Models for this derivative behaviour have been constructed, but they are completely *ad hoc* [4, 5]. We shall present a description of polarization, based on the recently perfected version of semiclassical theory, which includes these two types of behaviour (linear with angle or oscillatory) as special cases.

In the modern semiclassical theory, scattering is described with a classical trajectory for the projectile together with a quantum phase for the particle on the trajectory. In cases of interest, there are two dominant trajectories leading from the incident beam direction to a given scattering angle. These trajectories pass each side of the nucleus, and their interference gives rise to the diffractive structure. Such a theory is well-suited to a simplified description of polarization phenomena, since the spin-dependent potential will differ along the two trajectories on opposite sides of the nucleus.

The remainder of this paper is organized as follows. In section 2 we recall the main results of the semiclassical method, together with some useful analytic approximations, and apply it to polarization. The main result is eqs. (2.20-2.21). In section 3 we compare the results with optical model calculations and experimental data. In section 4 we examine previous models, and summarize the results.

(*) Supported by the National Science Foundation under Grant No. PHY76-20097 A01.

IMPLICATIONS OF EXPERIMENTAL MAGNETIC
MOMENT VALUES IN LIGHT NUCLEI FOR
THE PRESENCE AND CHARACTERISTICS OF
MESONIC EXCHANGE CURRENTS

B.H. WILDENTHAL¹

*Gesellschaft für Schwerionenforschung
6100 Darmstadt, Germany*

and

*Cyclotron Laboratory, Michigan State University**
E. Lansing, Michigan 48824, USA*

W. CHUNG

*Cyclotron Laboratory, Michigan State University**
E. Lansing, Michigan 48824, USA*

CONTENTS

1. Introduction 723
 2. Alternate analyses of magnetic moments 723
 3. A shell model for $17 \leq A \leq 39$ nuclei 727
 4. Experimental magnetic moments in the region $17 \leq A \leq 39$ 734
 5. Shell model analysis of experimental magnetic moments 734
- References 752

¹Fellow of the John Simon Guggenheim Memorial Foundation, 1977.

*Permanent address.

**Supported in part by the US National Science Foundation.

Mesons in Nuclei

Eds. M. Rho and D.H. Wilkinson

© North-Holland Publishing Company, 1979

COURSE 3

DYNAMICS OF HEAVY ION COLLISIONS*

George F. BERTSCH

*Physics Department, Cyclotron Laboratory, Michigan State University,
East Lansing, Mich. 48824, USA*

* Supported by the National Science Foundation.

*R. Balian et al., eds.
Les Houches, Session XXX, 1977. Ions lourds et mésons en physique nucléaire| Nuclear
physics with heavy ions and mesons
© North-Holland Publishing Company, 1978*